Electronic Supplementary Material (ESI) for ChemComm.

Supporting information

An Indicator Displacement Assay Recognizes Enantiomers of Chiral Carboxylates

Sara Sheykhi,[a] Lorenzo Mosca,[b] Johnathon M. Durgala,[a] and Pavel Anzenbacher, Jr.[a],*

[a] Department of Chemistry, Bowling Green State University Bowling Green, OH 43403, USA
[b] Department of Chemistry, Northwestern University, Evanston, IL, 60208, USA

E-mail: pavel@bgsu.edu

Table of Contents

1. Chemicals and Instrumentation

All chemicals and solvents were analytical grade and they were used without purification. ^{1}H- and ^{13}C-NMR spectra were measured with a Bruker® Avance IITM 500MHz UltraShield™ (Bruker Corporation, Mass., USA) spectrometer operating at 11.7 T. The chemical shifts (δ ppm) are referenced to the respective solvent and splitting patterns are designed as s (singlet), d (doublet), t (triplet), m (multiplet). Mass-spectrometry studies were performed using a Shimadzu MS-8030 equipped with an electron spray ionization (ESI) source and a triple quadrupole mass analyzer or a Shimadzu Axima Performance Matrix assisted laser desorption ionization-time of flight (MALDI-TOF) mass spectrometer. The quantum yields were recorded by using a Hamamatsu Quantaurus QY-C11347 absolute quantum yield integrating sphere. The pH values of the solvent was measured with a Titrator T50 (Mettler Toledo Co.). All titrations and enantiomeric excess calibration curves were measured at 25°C in a 7:3 CH_3CN:H_2O solution, buffered to pH=6 with 50 mM MES. Fluorescence measurements were performed on a single photon counting spectrofluorimeter from Edinburgh Analytical Instruments (FL/FS 920). Solutions of copper-based chiral sensors were excited at 444 nm. Fluorescence emission spectra were recorded between 455 nm and 600 nm. The band passes of excitation and emission monochromators were set to 1.0 nm. The emission from probes was scanned in 1 nm steps. The dwell time was 0.20 sec. Scans were taken under ambient room conditions. Guest titrations were performed in CH_3CN:H_2O (7:3, v/v). Titration isotherms were constructed from changes in the fluorescence maximum at 492 nm. All errors of binding constants are < 20%.

2. Synthesis

2.1 Synthesis of (1S,2S)-diphenyl-N¹,N²-bis(quinolin-2-ylmethylene)ethane-1,2-diamine and (1R,2R)-diphenyl-N¹,N²-bis(quinolin-2-ylmethylene)ethane-1,2-diamine (1).

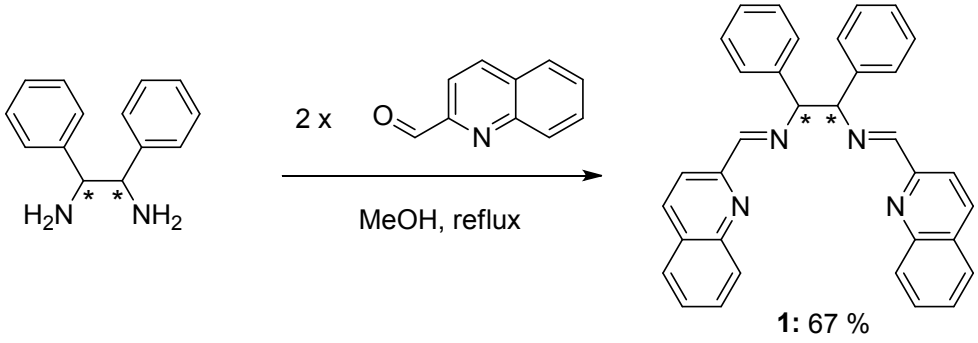

2-Quinolinecarboxaldehyde (222 mg, 1.41 mmol) was suspended in 10 mL of methanol and (*1S*,*2S*)-diphenylethylenediamine or (*1R*,*2R*)-diphenylethylenediamine (150 mg, 0.706 mmol) was added. The mixture was stirred and refluxed for 12 hours. After this time the reaction mixture was cooled down to room temperature and the yellow precipitate was collected by filtration and washed with diethyl ether. The pale-yellow solid was dried in air. The resulting crude material was recrystallized from ethyl acetate to give **1** as a white solid. (232 mg, 0.473 mmol, yield: 67%).

(1S,2S)-diphenyl-N¹,N²-bis(quinolin-2-ylmethylene)ethane-1,2-diamine (^{SS}L): ^{1}H NMR (500MHz, $CDCl_3$): δ = 8.41 (s, 2H), 8.04 (d, *J* = 8.5Hz, 2H), 7.99 (d, *J* = 8.5Hz, 2H), 7.75 (d, *J* = 7.9Hz, 2H), 7.68 (m, 6H), 7.64 (ddd, *J* = 8.3, 6.9, 1.3Hz, 2H), 7.48 (m, 2H), 7.34 (m, 6H), 5.48 (s, 2H) ppm.

^{13}C NMR (125 MHz, $CDCl_3$): δ 162.50, 160.55, 147.42, 136.21, 135.71, 130.70, 129.24, 129.04, 128.42, 128.40, 127.62, 127.47, 126.05, 121.81, 82.11 ppm.

MALDI-TOF (m/z): 491.20 [***M***+H]$^+$

(1R,2R)-diphenyl-N¹,N²-bis(quinolin-2-ylmethylene)ethane-1,2-diamine (^{RR}L): ^{1}H NMR (500MHz, $CDCl_3$): δ 8.40 (s, 2H), 8.04 (d, *J* = 8.5 Hz, 2H), 7.99 (d, *J* = 8.4 Hz, 2H), 7.75 (dd, *J* = 8.1, 1.1 Hz, 2H), 7.68 (m, 6H), 7.64 (ddd, *J* = 8.4, 6.9, 1.4 Hz, 2H), 7.48 (ddd, J = 6.9, 5.1, 1.1 Hz, 2H), 7.33 (m, 6H), 5.48 (s, 2H) ppm.

^{13}C NMR (125 MHz, $CDCl_3$): δ 162.49, 160.55, 147.42, 136.21, 135.71, 130.69, 129.24, 129.03, 128.41, 128.40, 127.61, 127.47, 126.04, 121.81, 82.11 ppm.

MALDI-TOF (m/z): 491.30 [***M***+H]$^+$

2.2 Synthesis of (1S,2S)-diphenyl-N^1,N^2-bis(quinolin-2-ylmethyl)ethane-1,2-diamine and (1R,2R)-diphenyl-N^1,N^2-bis(quinolin-2-ylmethyl)ethane-1,2-diamine (^{SS}L or ^{RR}L).

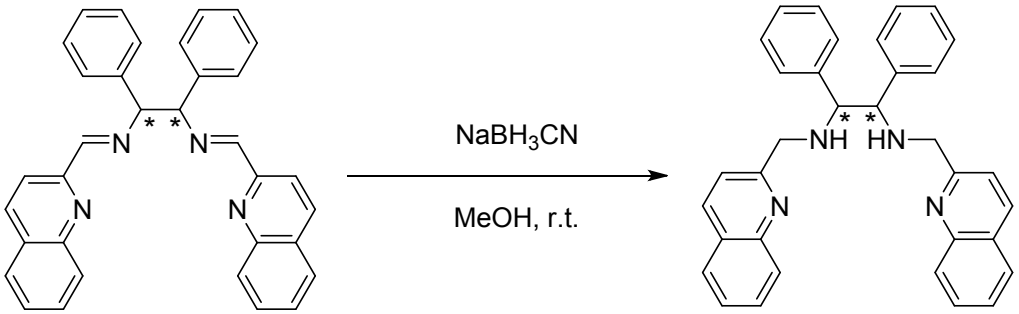

L: 96 %

The Schiff base (200 mg, 0.408 mmol) was suspended in 40 mL of methanol then 0.4mL acetic acid was added to the solution. Sodium cyanoborohydride (128 mg, 2.04 mmol) was added to the reaction mixture in portion wise (32 mg x 4 times) and the solution was stirred under a nitrogen atmosphere for 12 hours at room temperature. As the reaction progressed, the precipitate starts dissolving. After this time the reaction mixture was stirred and refluxed for additional 1 hour then cooled down to room temperature. Hydrochloric acid (1 mL, 2 M) was added to remove unreacted reducing reagent. The pH of the solution was adjusted (pH= 8) by the addition of concentrated Sodium hydroxide. The solvent was removed under reduced pressure and the residue was dissolved in 20 mL chloroform and filtered. The solvent removed in *vacuo* to yield yellow-brownish oil. (193 mg, 0.391 mmol, yield: 96%).

***(1S,2S)-diphenyl-N1,N2-bis(quinolin-2-ylmethyl)ethane-1,2-diamine* (^{SS}L):** ^{1}H NMR (500MHz, $CDCl_3$) : δ 8.11 (d, J = 8.4 Hz, 2H), 8.06 (d, J = 8.5 Hz, 2H), 7.80 (d, J = 8.1 Hz, 2H), 7.70 (ddd, J = 8.4, 5.5, 1.4 Hz, 2H), 7.51 (ddd, J = 8.1, 5.7, 1.1 Hz, 2H), 7.46 (d, J = 8.4 Hz, 2H), 7.41 (m, 4H), 7.34 (m, 4H), 7.27 (dt, J = 4.3, 1.7 Hz, 2H), 4.13 (s, 4H), 3.92 (s, 4H) ppm.

^{13}C NMR (125 MHz, $CDCl_3$): δ 162.36, 147.38, 140.51, 136.21, 129.22, 128.77, 128.57, 128.15, 127.51, 127.37, 126.68, 125.87, 120.72, 55.92, 54.05 ppm.

MALDI-TOF (m/z): 495.30 [***M***+H]$^+$

***(1R,2R)-diphenyl-N^1,N^2-bis(quinolin-2-ylmethyl)ethane-1,2-diamine* (^{RR}L)**: ^{1}H NMR (500MHz, $CDCl_3$) : δ 8.10 (d, J = 8.5 Hz, 2H), 8.02 (d, J = 8.5 Hz, 2H), 7.79 (m, 4H), 7.67 (ddd, J = 8.4, 6.9, 1.5 Hz, 2H), 7.48 (m, 2H), 7.39 (dd, J = 7.9, 1.0 Hz, 4H), 7.28 (dd, J = 10.7, 4.4 Hz, 6H), 7.20 (m, 2H), 3.92 (s, 4H), 3.65 (s, 4H) ppm.

^{13}C NMR (125 MHz, $CDCl_3$): δ 160.15, 147.72, 140.13, 136.41, 129.46, 128.96, 128.42, 128.32, 127.57, 127.29, 127.02, 126.06, 120.60, 55.06, 53.67 ppm.

MALDI-TOF (m/z): 495.30 [***M***+H]$^+$

***2.3 General procedure for the synthesis of ((1S,2S)-diphenyl-N1,N2-bis(quinolin-2-ylmethyl)ethane-1,2-diamine) copper(II)* $[Cu^{SS}L](OTf)_2$ *and ((1R,2R)-diphenyl-N1,N2-bis(quinolin-2-ylmethyl)ethane-1,2-diamine) copper(II)* $[Cu^{RR}L](OTf)_2$**

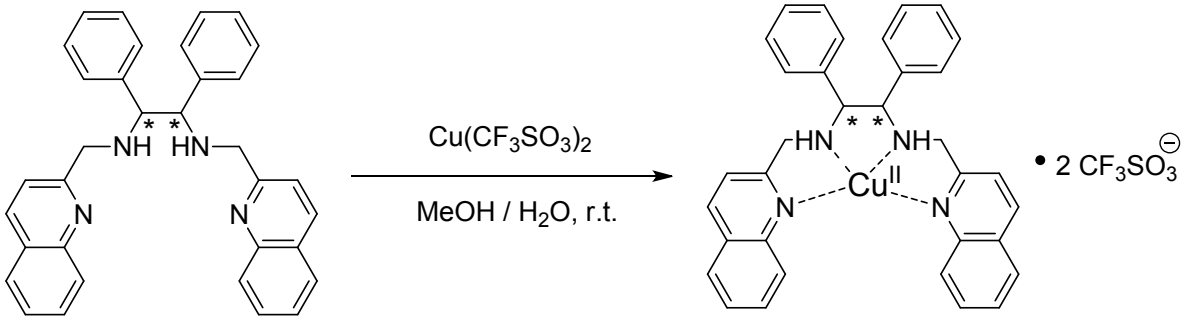

(L) **$[Cu^{RR}L]^{2+}$ or $[Cu^{SS}L]^{2+}$:** 98 %

In a 100 mL round-bottom flask, **L** (150 mg, 0.303 mmol) was dissolved in 30 mL of methanol under nitrogen. Copper (II) trifluoromethanesulfonate (110 mg, 0.303 mmol) was dissolved in 2 mL ultrapure water in a small vial. The two solutions were mixed and stirred under nitrogen for 12 hours. The solvent was removed in *vacuo* and the resulting green-bluish solid was dried under high vacuum for 2 hours. The product was washed with diethyl ether, filtered and dried in a desiccator (166 mg, 0.297 mmol, yield: 98 %).

MALDI-TOF (m/z): $[\boldsymbol{M}]^+$: 557.20

3. NMR spectra

Figure S1. ^{1}H NMR (500 MHz) of (*1S,2S*)-diphenyl-*N*^{1},*N*^{2}-bis(quinolin-2-ylmethylene)ethane-1,2-diamine in $CDCl_3$.

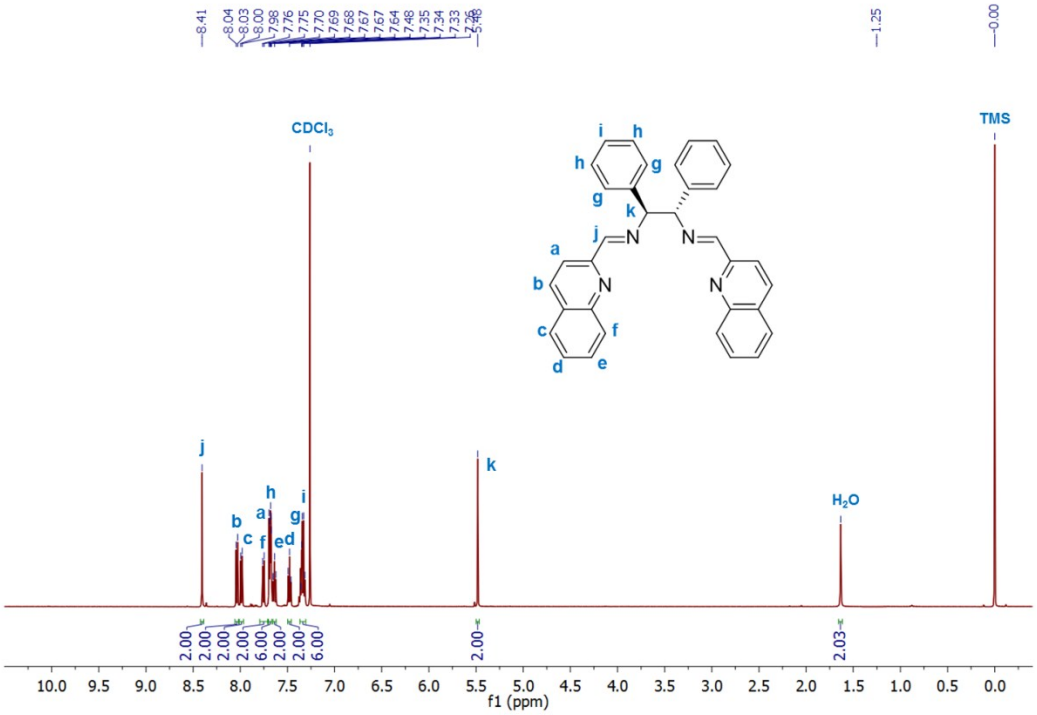

Figure S2. ^{13}C NMR (125 MHz) of (*1S,2S*)-diphenyl-*N*^{1},*N*^{2}-bis(quinolin-2-ylmethylene)ethane-1,2-diamine in $CDCl_3$.

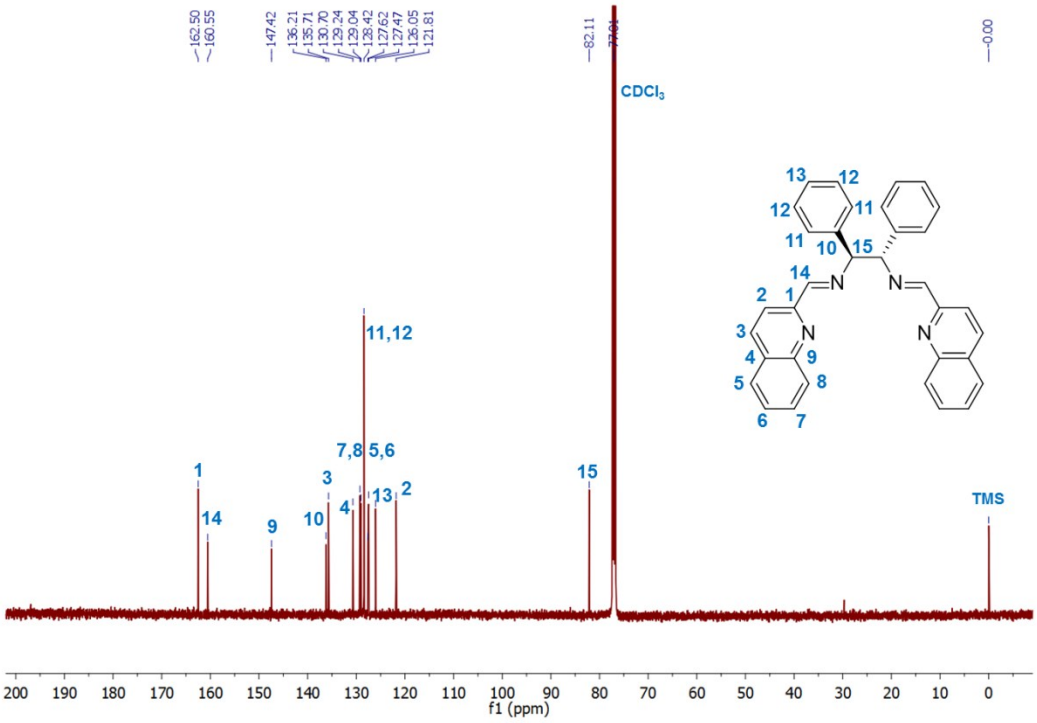

Figure S3. ^{1}H NMR (500 MHz) of (*1S,2S*)-diphenyl-*N*^{1},*N*^{2}-bis(quinolin-2-ylmethyl)ethane-1,2-diamine in $CDCl_3$.

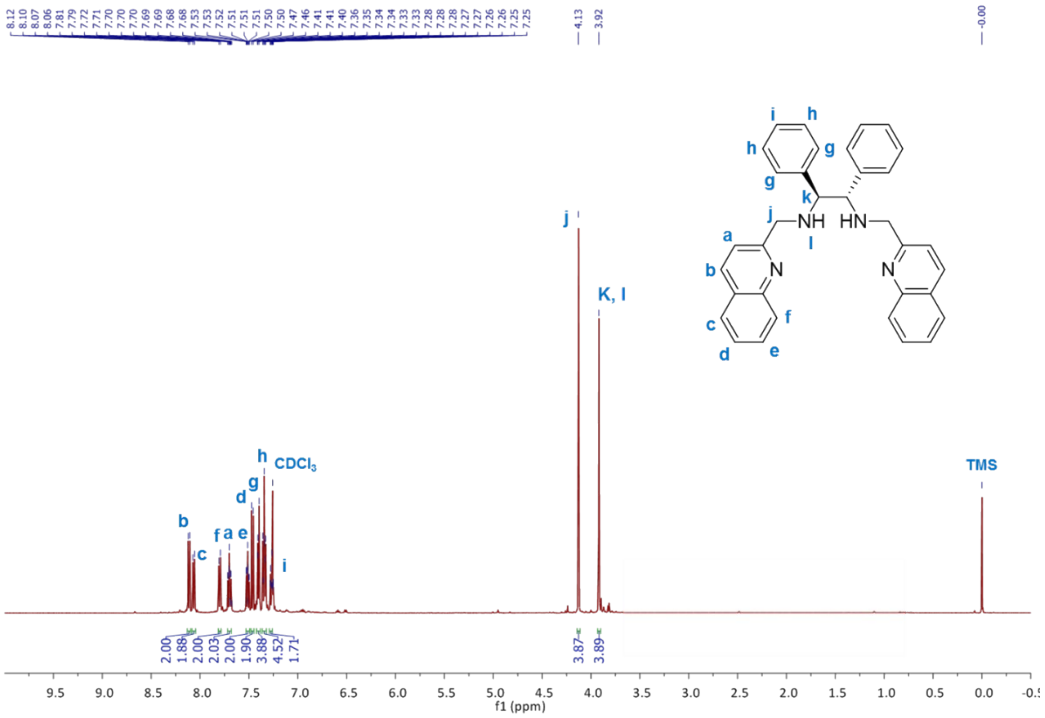

Figure S4. ^{13}C NMR (125 MHz) of (*1S,2S*)-diphenyl-*N*^{1},*N*^{2}-bis(quinolin-2-ylmethyl)ethane-1,2-diamine in $CDCl_3$.

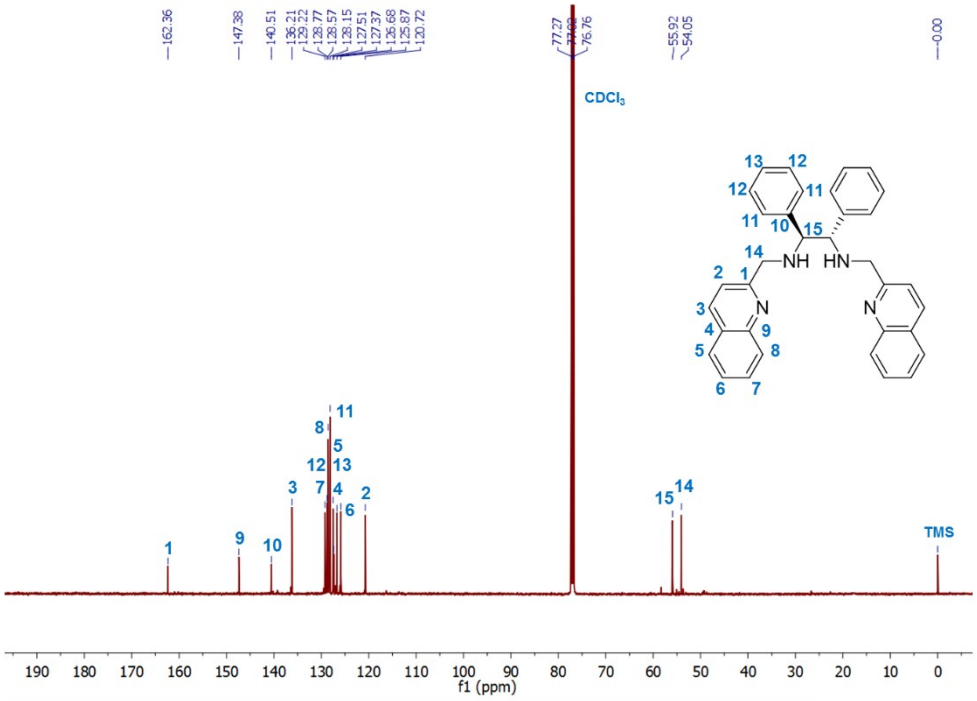

Figure S5. ^{1}H NMR (500 MHz) of (*1R,2R*)-diphenyl-*N*^{1},*N*^{2}-bis(quinolin-2-ylmethylene)ethane-1,2-diamine in $CDCl_3$.

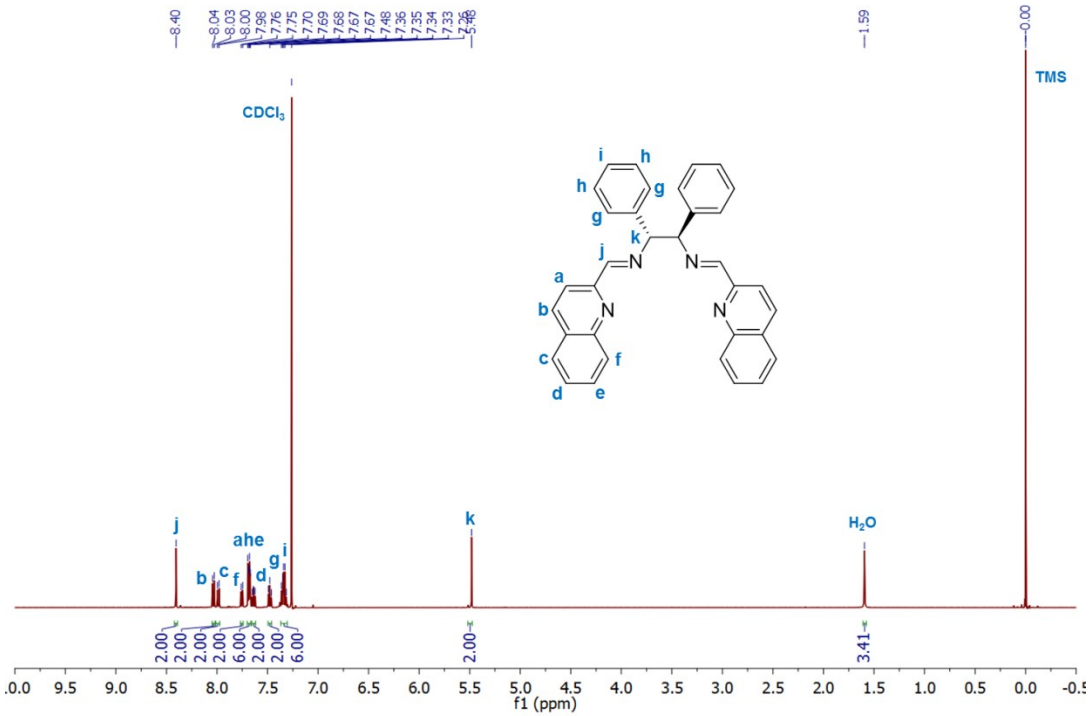

Figure S6. ^{13}C NMR (125 MHz) of (*1R,2R*)-diphenyl-*N*^{1},*N*^{2}-bis(quinolin-2-ylmethylene)ethane-1,2-diamine in $CDCl_3$.

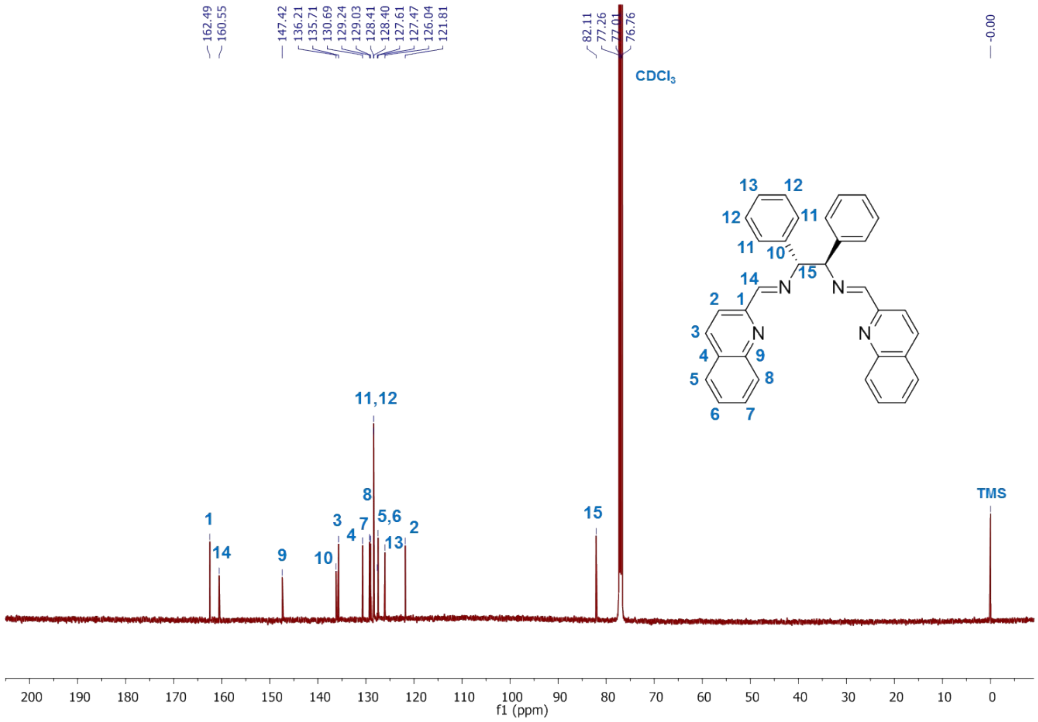

Figure S7. ^{1}H NMR (500 MHz) of (*1R,2R*)-diphenyl-*N*^{1},*N*^{2}-bis(quinolin-2-ylmethyl)ethane-1,2-diamine in $CDCl_3$.

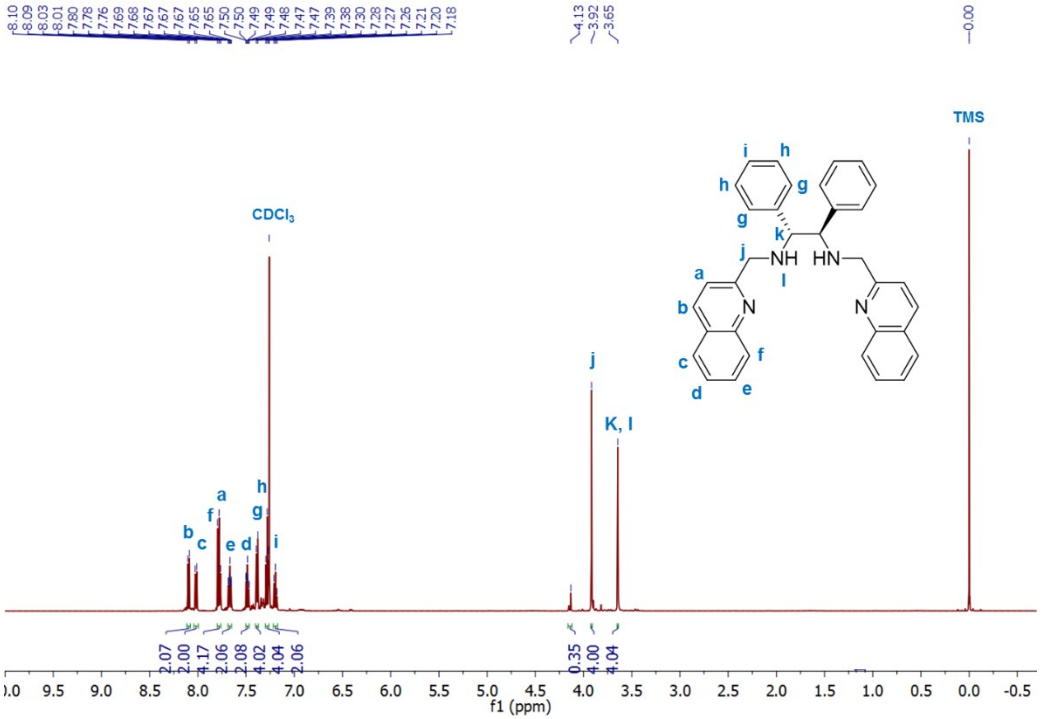

Figure S8. ^{13}C NMR (125 MHz) of (*1R,2R*)-diphenyl-*N*^{1},*N*^{2}-bis(quinolin-2-ylmethyl)ethane-1,2-diamine in $CDCl_3$.

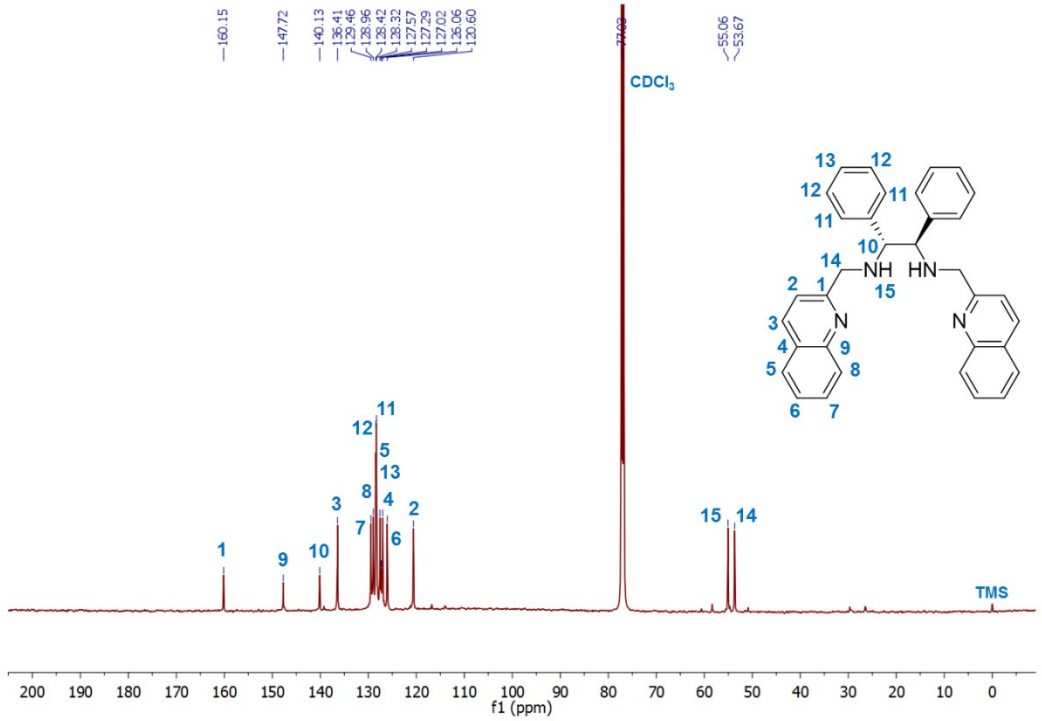

4. Mass Spectroscopy

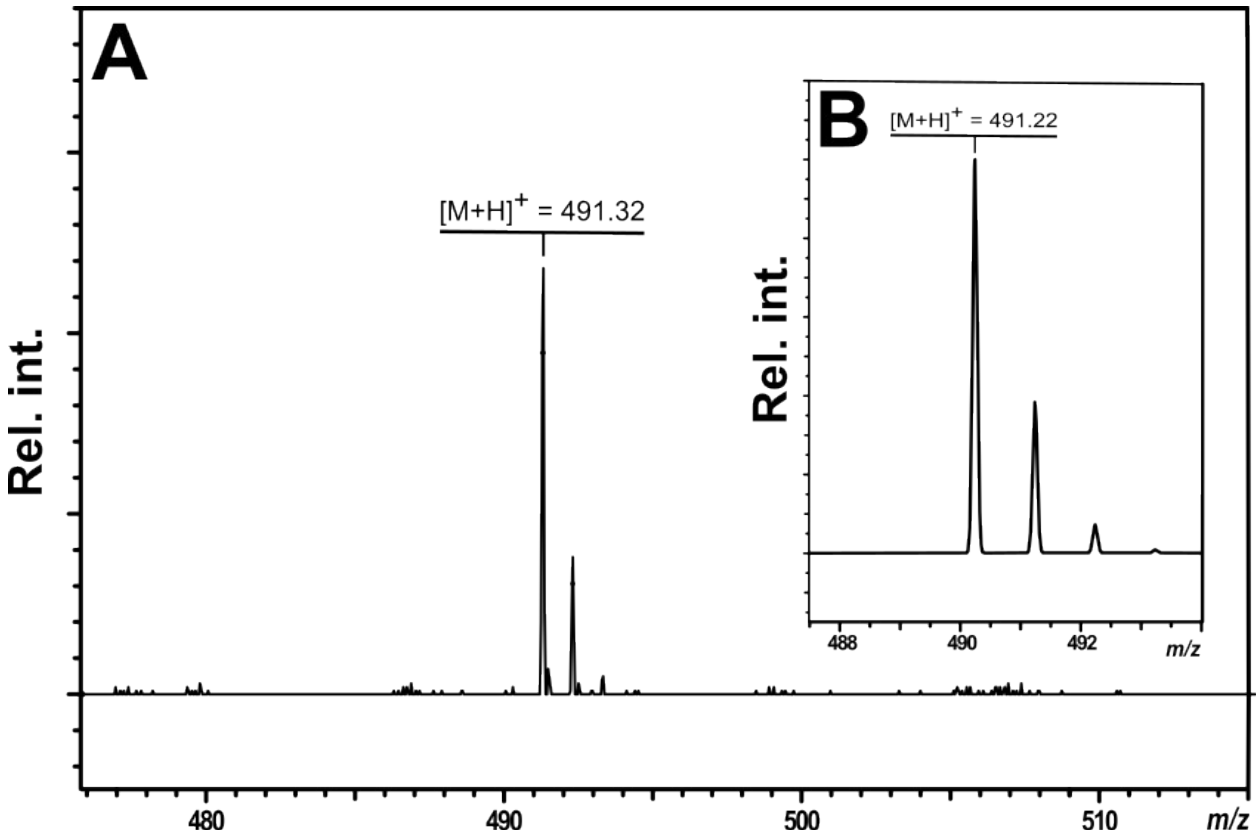

Figure S9. A: MALDI spectrum of (*1R,2R*)-diphenyl-N^1,N^2-bisquinolin-2-ylmethylene)ethane-1,2-diamine. **B:** Calculated isotope pattern for $\mathbf{C_{34}H_{26}N_4}$.

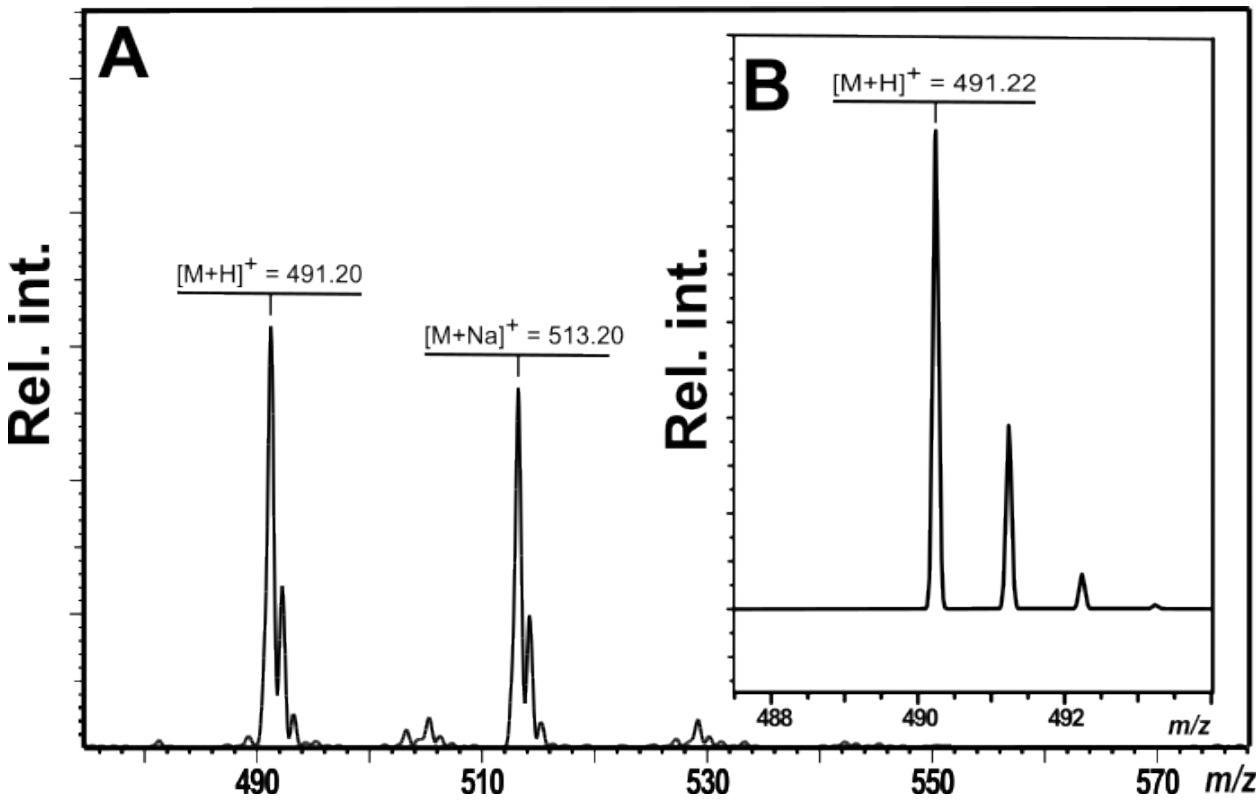

Figure S10. A: MALDI spectrum of (*1S,2S*)-diphenyl-N^1,N^2-bis(quinolin-2-ylmethylene)ethane-1,2-diamine. **B:** Calculated isotope pattern for $\mathbf{C_{34}H_{26}N_4}$.

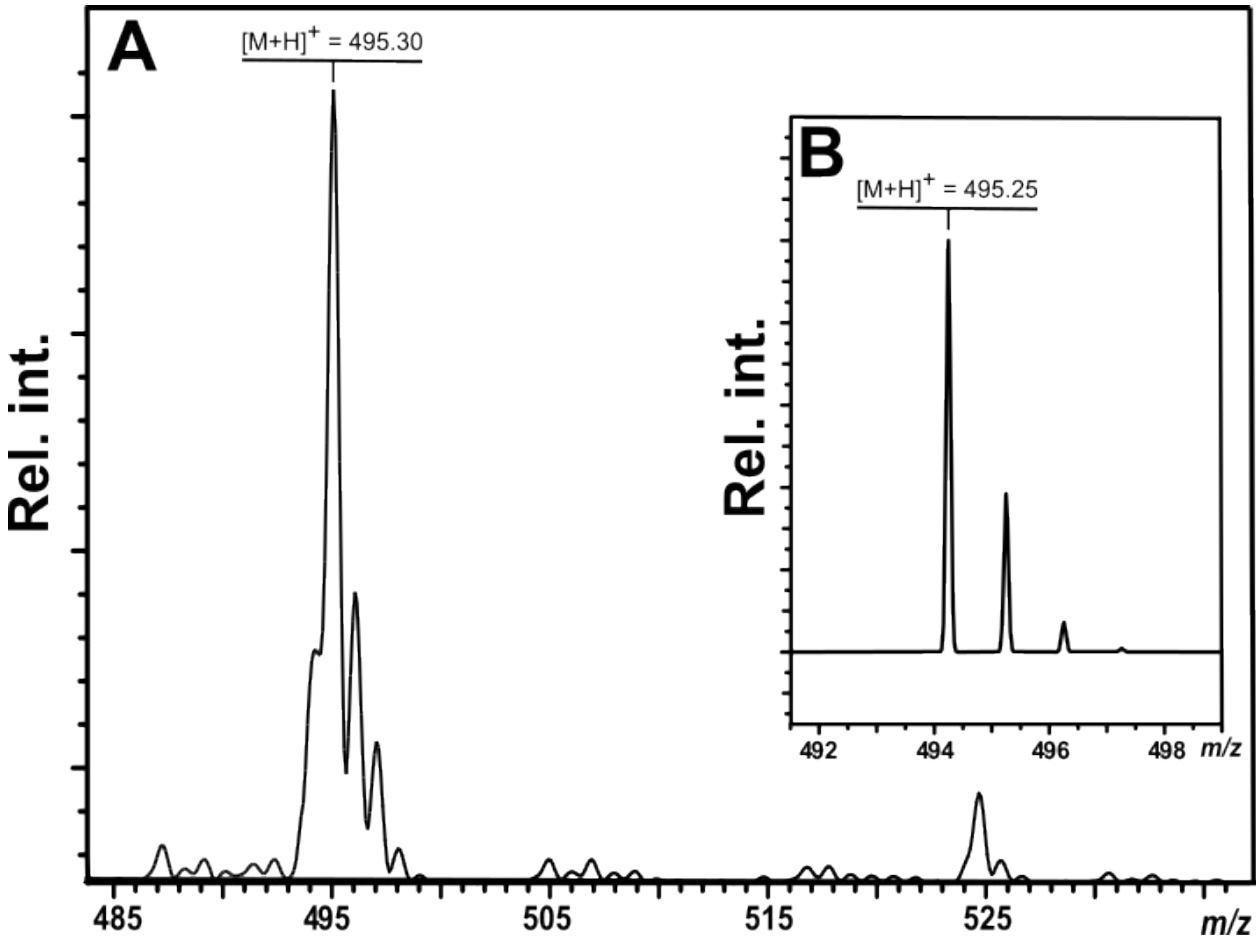
A
[M+H]+ = 495.30
Rel. int.
485
495
505
515
525
m/z
B
[M+H]+ = 495.25
Rel. int.
492
494
496
498
m/z

Figure S11. **A:** MALDI spectrum of *(1R,2R)*-diphenyl-N^1,N^2-bis(quinolin-2-ylmethyl)ethane-1,2-diamine. **B:** Calculated isotope pattern for $\mathbf{C_{34}H_{30}N_4}$.

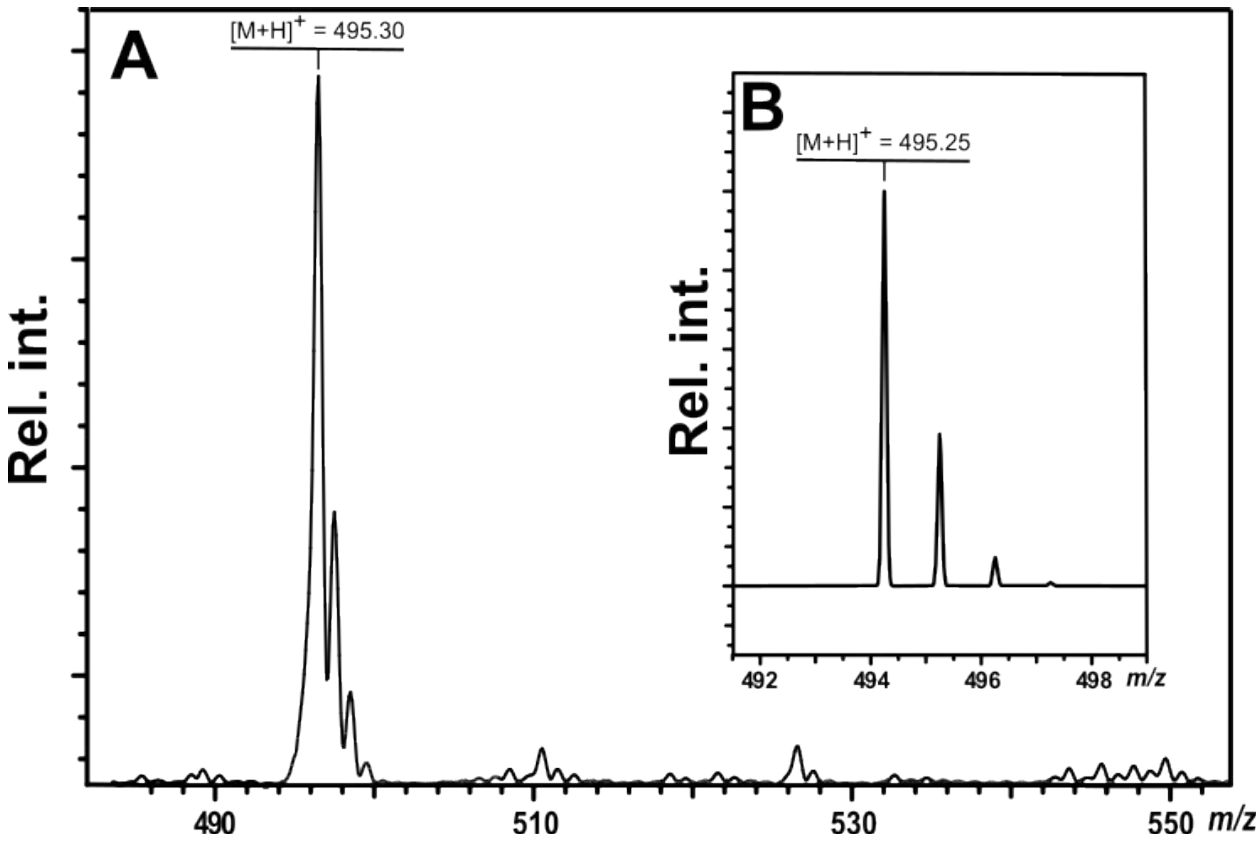

Figure S12. **A:** MALDI spectrum of *(1S,2S)*-diphenyl-N^1,N^2-bis(quinolin-2-ylmethyl)ethane-1,2-diamine. **B:** Calculated isotope pattern for $\mathbf{C_{34}H_{30}N_4}$.

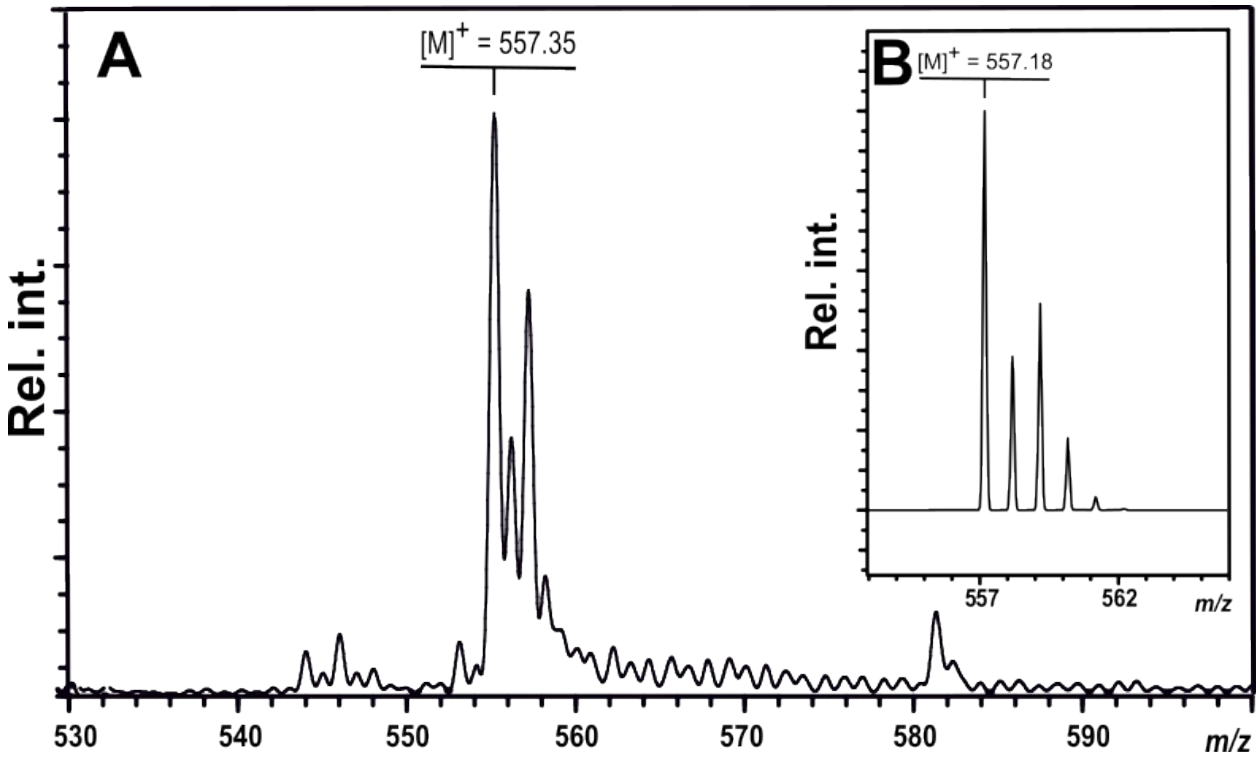

Figure S13. **A:** MALDI spectrum of ((*1R,2R*)-diphenyl-N^1,N^2-bis(quinolin-2-ylmethyl)ethane-1,2-diamine) copper(II) $[Cu^{RR}L]^{2+}$. **B:** Calculated isotope pattern for $\mathbf{C_{34}H_{30}CuN_4}$.

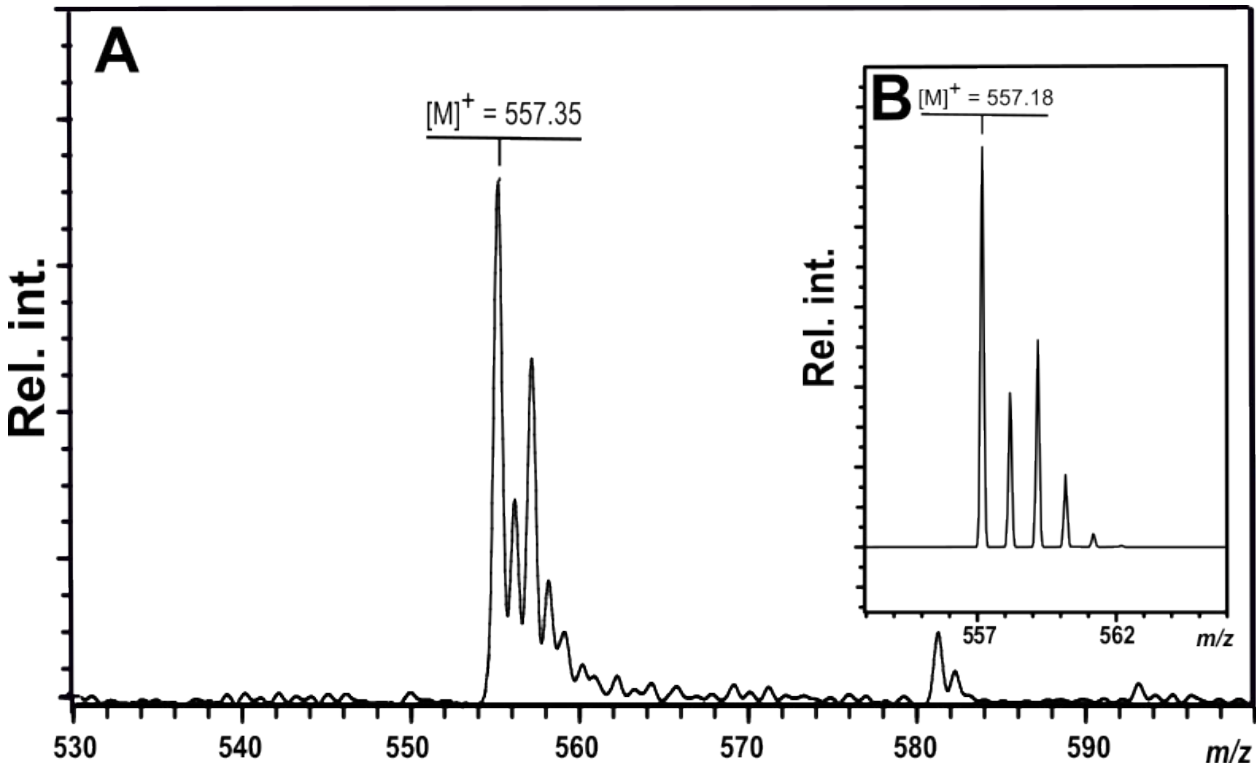

Figure S14. **A:** MALDI spectrum of ((*1S,2S*)-diphenyl-N^1,N^2-bis(quinolin-2-ylmethyl)ethane-1,2-diamine) copper(II) $[Cu^{SS}L]^{2+}$. **B:** Calculated isotope pattern for $\mathbf{C_{34}H_{30}CuN_4}$.

5. Fluorescence titrations

All solutions were prepared in CH_3CN:H_2O 7:3 at pH= 6 (MES 50 mM). The concentrations used were: [Sensors]= 212 μM, [C343]= 0.01 μM.

Control Experiment

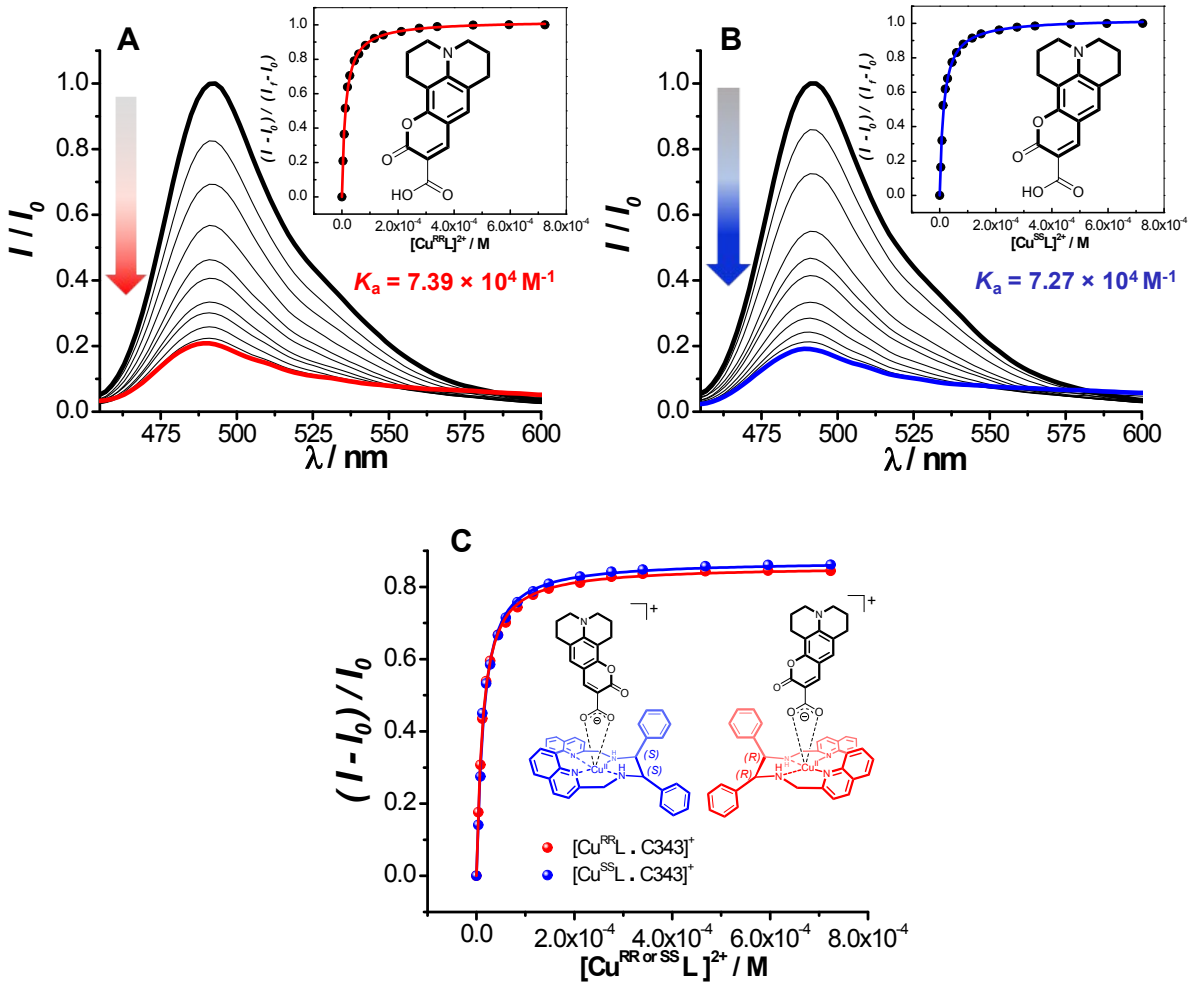

Figure S15. A) Fluorescence titration profiles of Coumarin 343 (0.01 μM) upon the addition of chiral receptors **[Cu^{SS}L]$^{2+}$** (blue); **B) [Cu^{RR}L]$^{2+}$** (red) in CH_3CN:H_2O 7:3 at pH= 6 (MES 50 mM); **C)** Titration isotherms based on the change in fluorescence intensity at the maximum wavelength of Coumarin 343 and partly quenched upon the addition of incremental amounts of **[Cu^{SS}L)]$^{2+}$** (blue) and **[Cu^{RR}L]$^{2+}$** (red). λ_{ex}= 444 nm. [**[Cu^{SS}L]$^{2+}$**] = [**[Cu^{RR}L]$^{2+}$**]= 0–800 μM.

[Cu^{SS}L•C343]$^{+}$ – Phenylpropionic acid

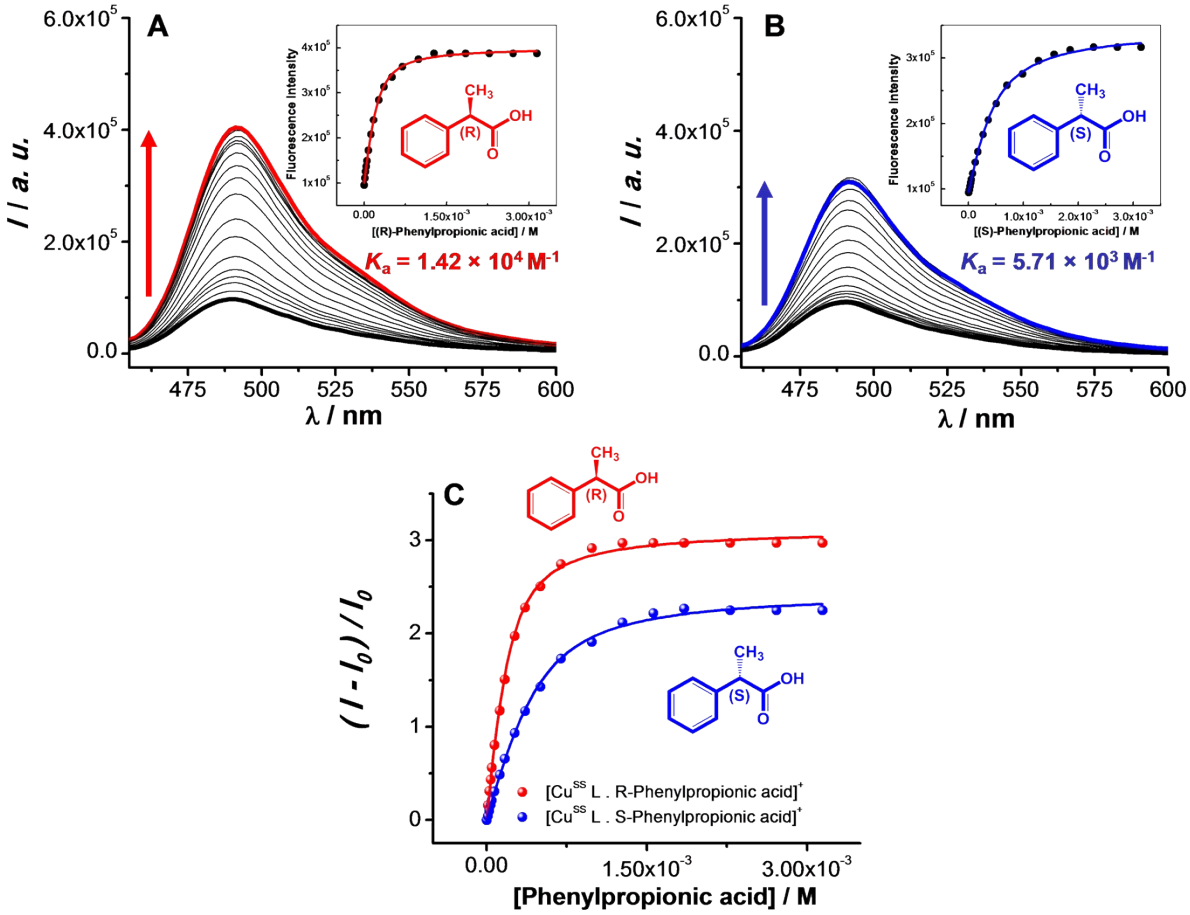

Figure S16. A) Titration profile of **[Cu^{SS}L•C343]$^{+}$** (212 μM) upon the addition of incremental amounts of **(*R*)-phenylpropionic acid** in CH_3CN:H_2O 7:3 at pH= 6 (MES 50 mM). λ_{ex}= 444 nm. [(*R*)-phenylpropionic acid]= 0–3 mM.

B) Titration profile of **[Cu^{SS}L•C343]$^{+}$** (212 μM) upon the addition of incremental amounts of **(*S*)-phenylpropionic acid** in CH_3CN:H_2O 7:3 at pH= 6 (MES 50 mM). λ_{ex}= 444 nm. [(*S*)-phenylpropionic acid]= 0–3 mM.

C) Titration isotherms based on the change in fluorescence intensity at the maximum wavelength of **[Cu^{SS}L•C343]$^{+}$** (212 μM) and partly enhanced upon the addition of incremental amounts of **(*R*)-phenylpropionic acid** (red) and **(*S*)-phenylpropionic acid** (blue) in CH_3CN:H_2O 7:3 at pH= 6 (MES 50 mM). λ_{ex}= 444 nm. [(*S*)/(*R*)-phenylpropionic acid]= 0–3 mM.

[Cu^{RR}L•C343]$^{+}$ – Phenylpropionic acid

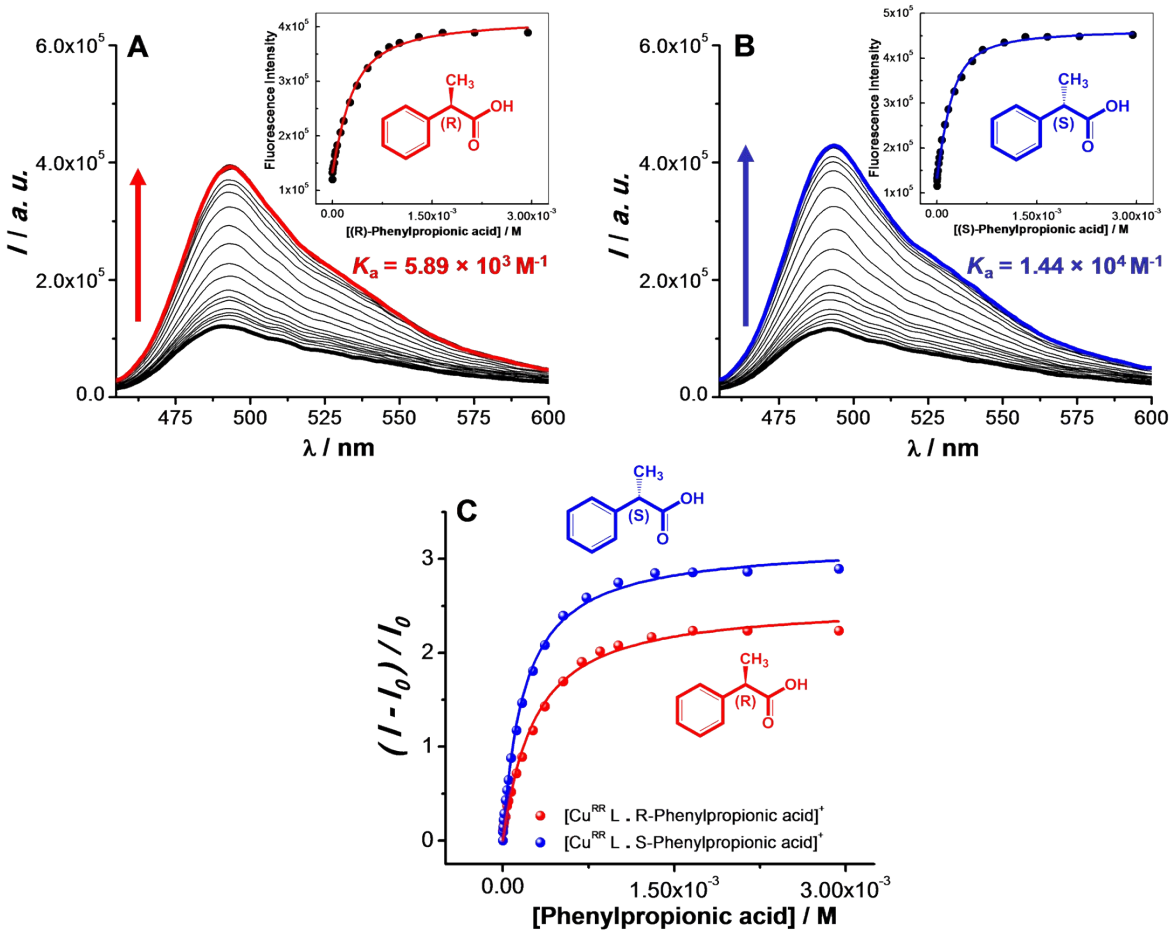

Figure S17. A) Titration profile of **[Cu^{RR}L•C343]$^{+}$** (212 μM) upon the addition of incremental amounts of **(*R*)-phenylpropionic acid** in CH_3CN:H_2O 7:3 at pH= 6 (MES 50 mM). λ_{ex}= 444 nm. [(*R*)-phenylpropionic acid]= 0–3 mM.

B) Titration profile of **[Cu^{RR}L•C343]$^{+}$** (212 μM) upon the addition of incremental amounts of **(*S*)-phenylpropionic acid** in CH_3CN:H_2O 7:3 at pH= 6 (MES 50 mM). λ_{ex}= 444 nm. [(*S*)-phenylpropionic acid]= 0–3 mM.

C) Titration isotherms based on the change in fluorescence intensity at the maximum wavelength of **[Cu^{RR}L•C343]$^{+}$** (212 μM) and partly enhanced upon the addition of incremental amounts of **(*R*)-phenylpropionic acid** (red) and **(*S*)-phenylpropionic acid** (blue) in CH_3CN:H_2O 7:3 at pH= 6 (MES 50 mM). λ_{ex} = 444 nm. [(*S*)/(*R*)-phenylpropionic acid]= 0–3 mM.

[Cu^{SS}L•C343]$^{+}$ – Ibuprofen

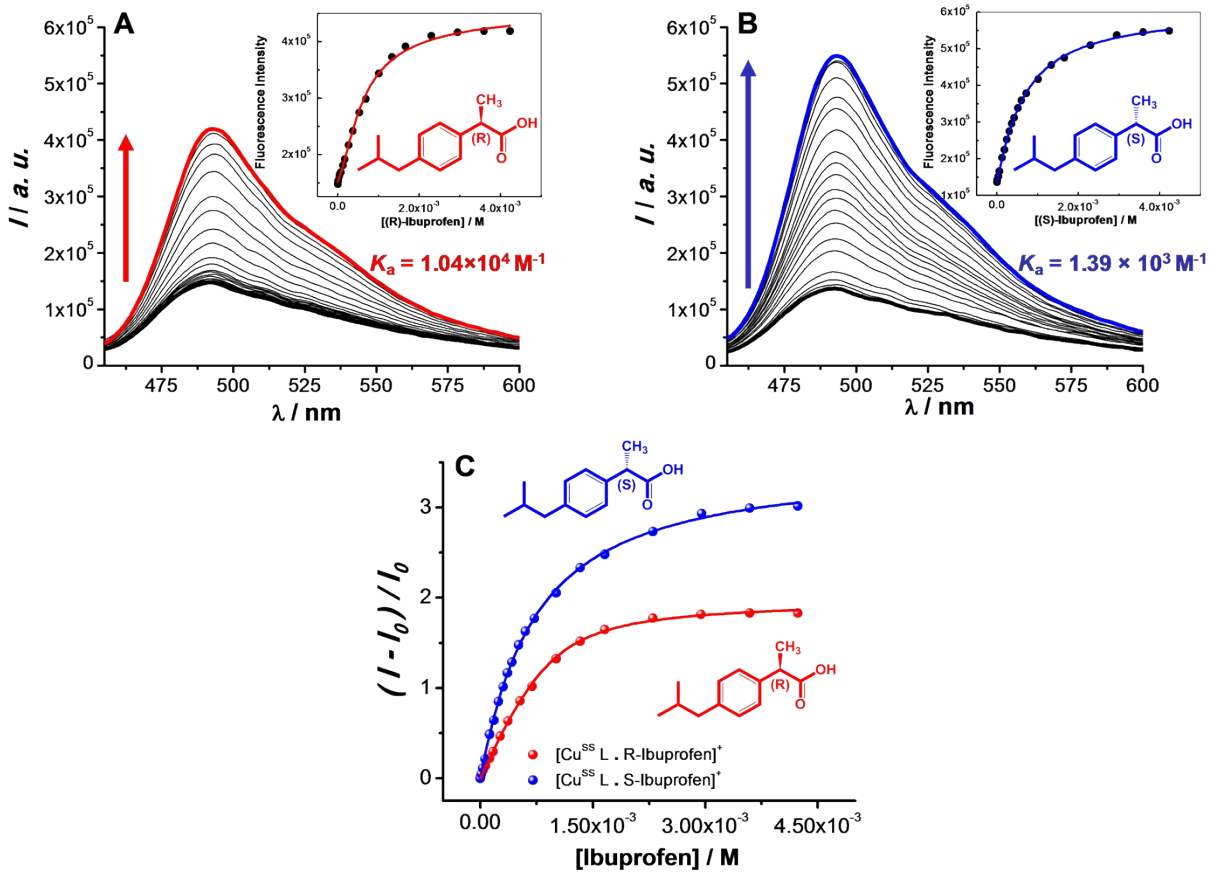

Figure S18. A) Titration profile of **[Cu^{SS}L•C343]**$^{+}$ (212 μM) upon the addition of incremental amounts of **(*R*)-Ibuprofen** in CH_3CN:H_2O 7:3 at pH= 6 (MES 50 mM). λ_{ex}= 444 nm. [(*R*)-Ibuprofen]= 0–4 mM.

B) Titration profile of **[Cu^{SS}L•C343]**$^{+}$ (212 μM) upon the addition of incremental amounts of **(*S*)-Ibuprofen** in CH_3CN:H_2O 7:3 at pH= 6 (MES = 50 mM). λ_{ex}= 444 nm. [(*S*)-Ibuprofen]= 0–4 mM.

C) Titration isotherms based on the change in fluorescence intensity at the maximum wavelength of **[Cu^{SS}L•C343]**$^{+}$ (212 μM) and partly enhanced upon the addition of incremental amounts of **(*R*)-Ibuprofen** (red) and **(*S*)-Ibuprofen** (blue) in CH_3CN:H_2O 7:3 at pH= 6 (MES 50 mM). λ_{ex} = 444 nm. [(*S*)/(*R*)-Ibuprofen]= 0–4 mM.

[Cu^{RR}L•C343]$^{+}$ – Ibuprofen

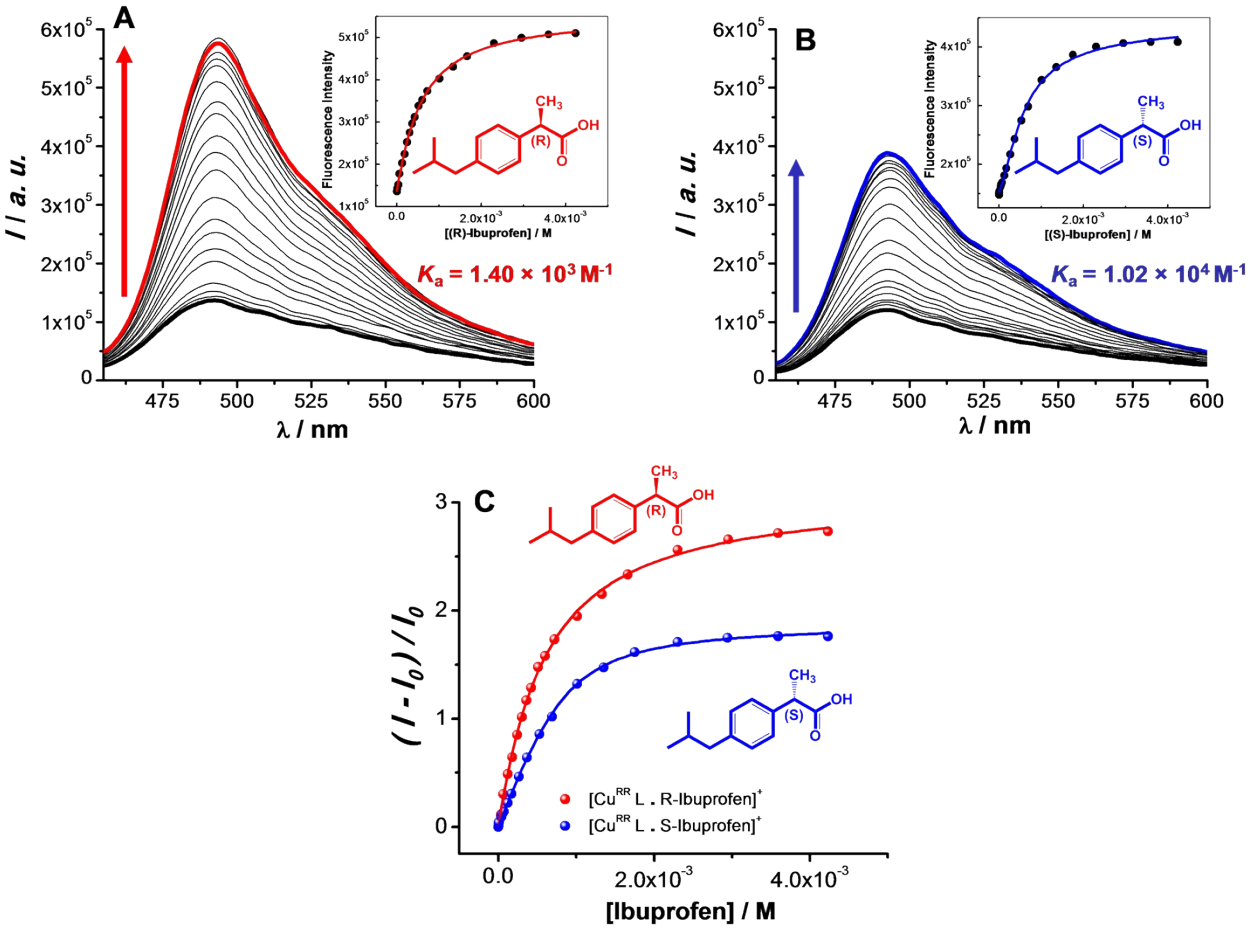

Figure S19. A) Titration profile of **[Cu^{RR}L•C343]**$^{+}$ (212 μM) upon the addition of incremental amounts of **(*R*)-Ibuprofen** in CH_3CN:H_2O 7:3 at pH= 6 (MES 50 mM). λ_{ex} = 444 nm. [(*R*)-Ibuprofen]= 0–4 mM.

B) Titration profile of **[Cu^{RR}L•C343]**$^{+}$ (212 μM) upon the addition of incremental amounts of **(*S*)-Ibuprofen** in CH_3CN:H_2O 7:3 at pH= 6 (MES 50 mM). λ_{ex}= 444 nm. [(*S*)-Ibuprofen]= 0–4 mM.

C) Titration isotherms based on the change in fluorescence intensity at the maximum wavelength of **[Cu^{RR}L•C343]**$^{+}$ (212 μM) and partly enhanced upon the addition of incremental amounts of **(*R*)-Ibuprofen** (red) and **(*S*)-Ibuprofen** (blue) in CH_3CN:H_2O 7:3 at pH= 6 (MES 50 mM). λ_{ex}= 444 nm. [(*S*)/(*R*)-Ibuprofen]= 0–4 mM.

[Cu^{SS}L•C343]$^{+}$ – Naproxen

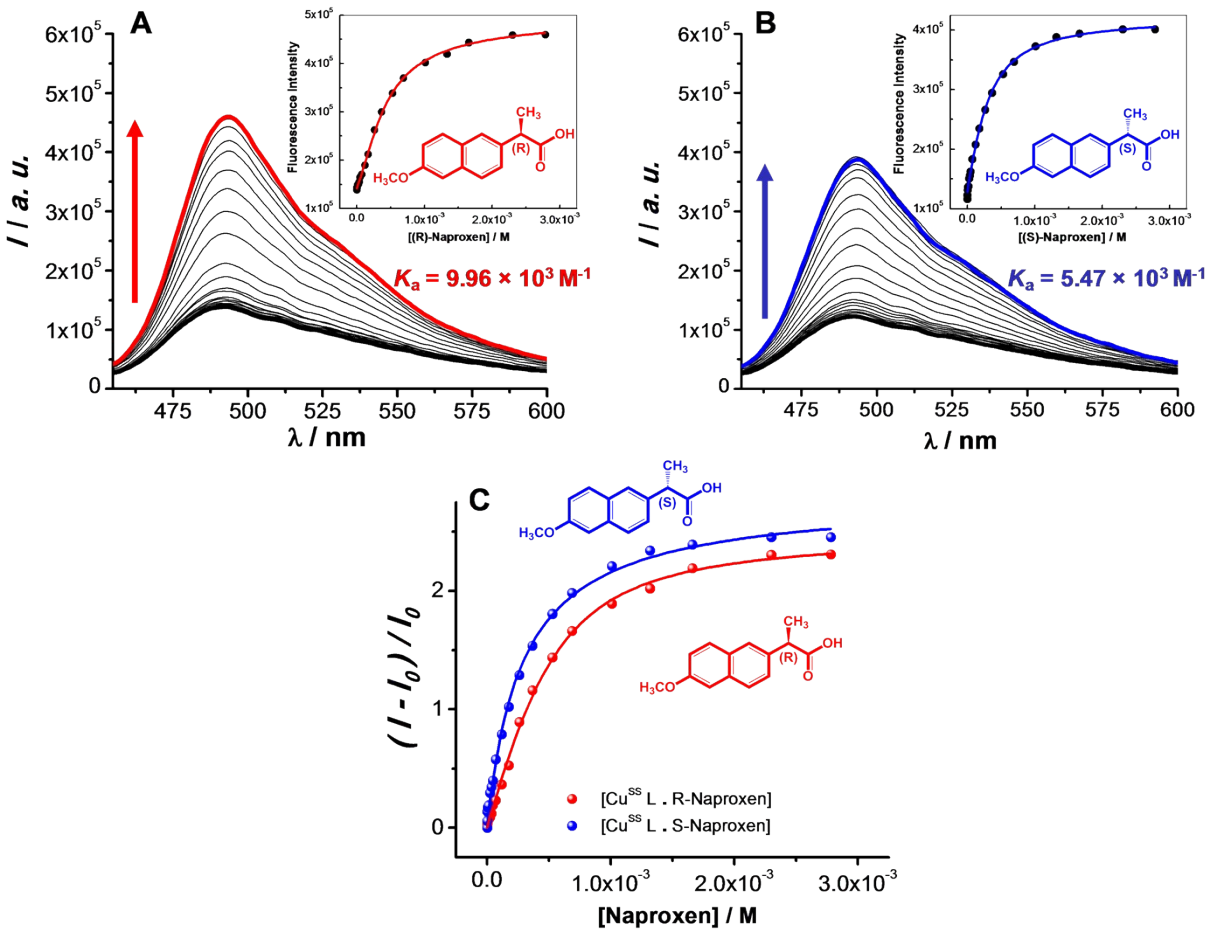

Figure S20. A) Titration profile of **[Cu^{SS}L•C343]$^{+}$** (212 μM) upon the addition of incremental amounts of **(*R*)-Naproxen** in CH_3CN:H_2O 7:3 at pH= 6 (MES 50 mM). λ_{ex}= 444 nm. [(*R*)-Naproxen]= 0–3 mM.

B) Titration profile of **[Cu^{SS}L•C343]$^{+}$** (212 μM) upon the addition of incremental amounts of **(*S*)-Naproxen** in CH_3CN:H_2O 7:3 at pH= 6 (MES 50 mM). λ_{ex}= 444 nm. [(*S*)-Naproxen]= 0–3 mM.

C) Titration isotherms based on the change in fluorescence intensity at the maximum wavelength of **[Cu^{SS}L•C343]$^{+}$** (212 μM) and partly enhanced upon the addition of incremental amounts of **(*R*)-Naproxen** (red) and **(*S*)-Naproxen** (blue) in CH_3CN:H_2O 7:3 at pH= 6 (MES 50 mM). λ_{ex}= 444 nm. [(*S*)/(*R*)-Naproxen]= 0–3 mM.

[Cu^{RR}L•C343]$^{+}$ – Naproxen

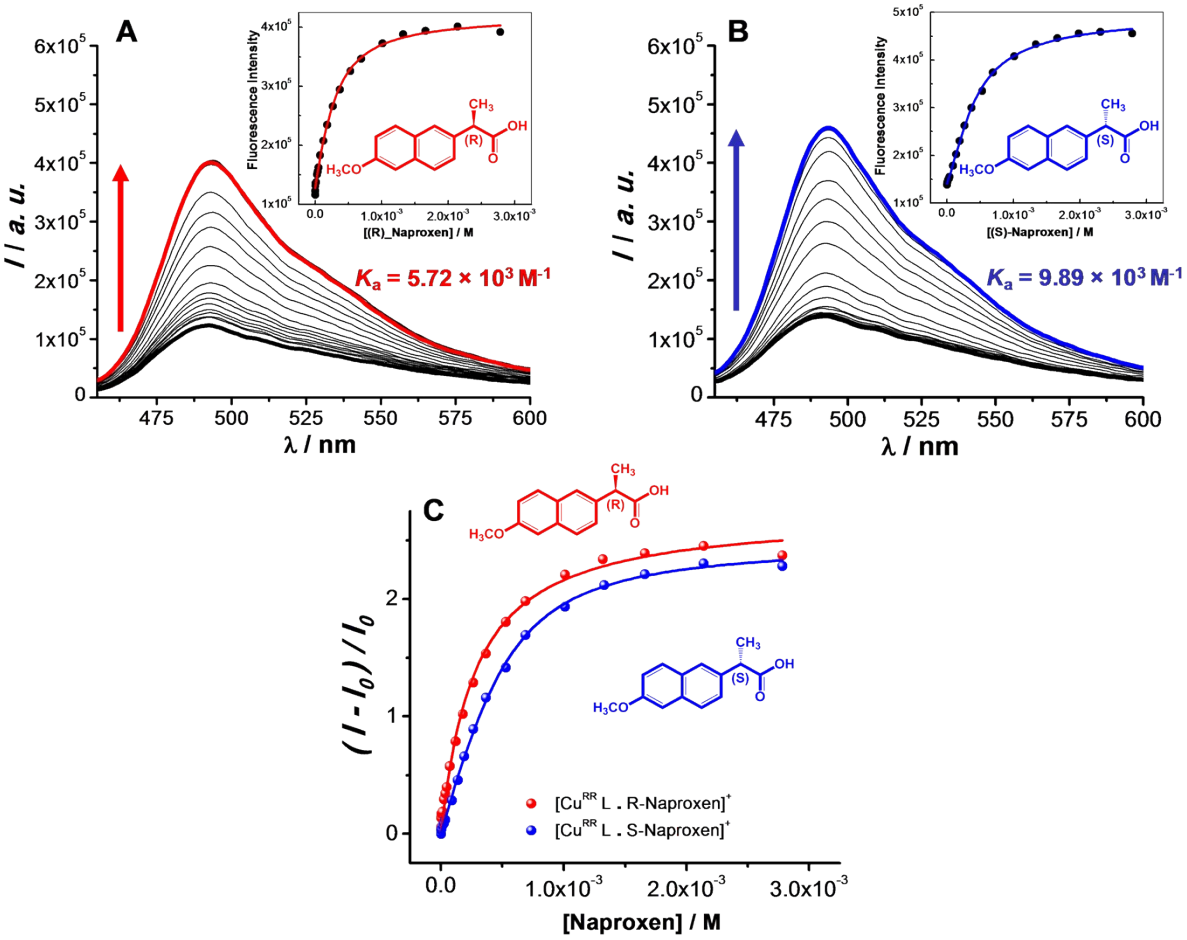

Figure S21. A) Titration profile of **[Cu^{RR}L•C343]$^{+}$** (212 μM) upon the addition of incremental amounts of **(*R*)-Naproxen** in CH_3CN:H_2O 7:3 at pH= 6 (MES 50 mM). λ_{ex}= 444 nm. [(*R*)-Naproxen]= 0–3 mM.

B) Titration profile of **[Cu^{RR}L•C343]$^{+}$** (212 μM) upon the addition of incremental amounts of **(*S*)-Naproxen** in CH_3CN:H_2O 7:3 at pH= 6 (MES 50 mM). λ_{ex}= 444 nm. [(*S*)-Naproxen]= 0–3 mM.

C) Titration isotherms based on the change in fluorescence intensity at the maximum wavelength of **[Cu^{RR}L•C343]$^{+}$** (212 μM) and partly enhanced upon the addition of incremental amounts of **(*R*)-Naproxen** (red) and **(*S*)-Naproxen** (blue) in CH_3CN:H_2O 7:3 at pH= 6 (MES 50 mM). λ_{ex}= 444 nm. [(*S*)/(*R*)-Naproxen]= 0–3 mM.

[Cu^{SS}L•C343]$^{+}$ – Atorvastatin Calcium

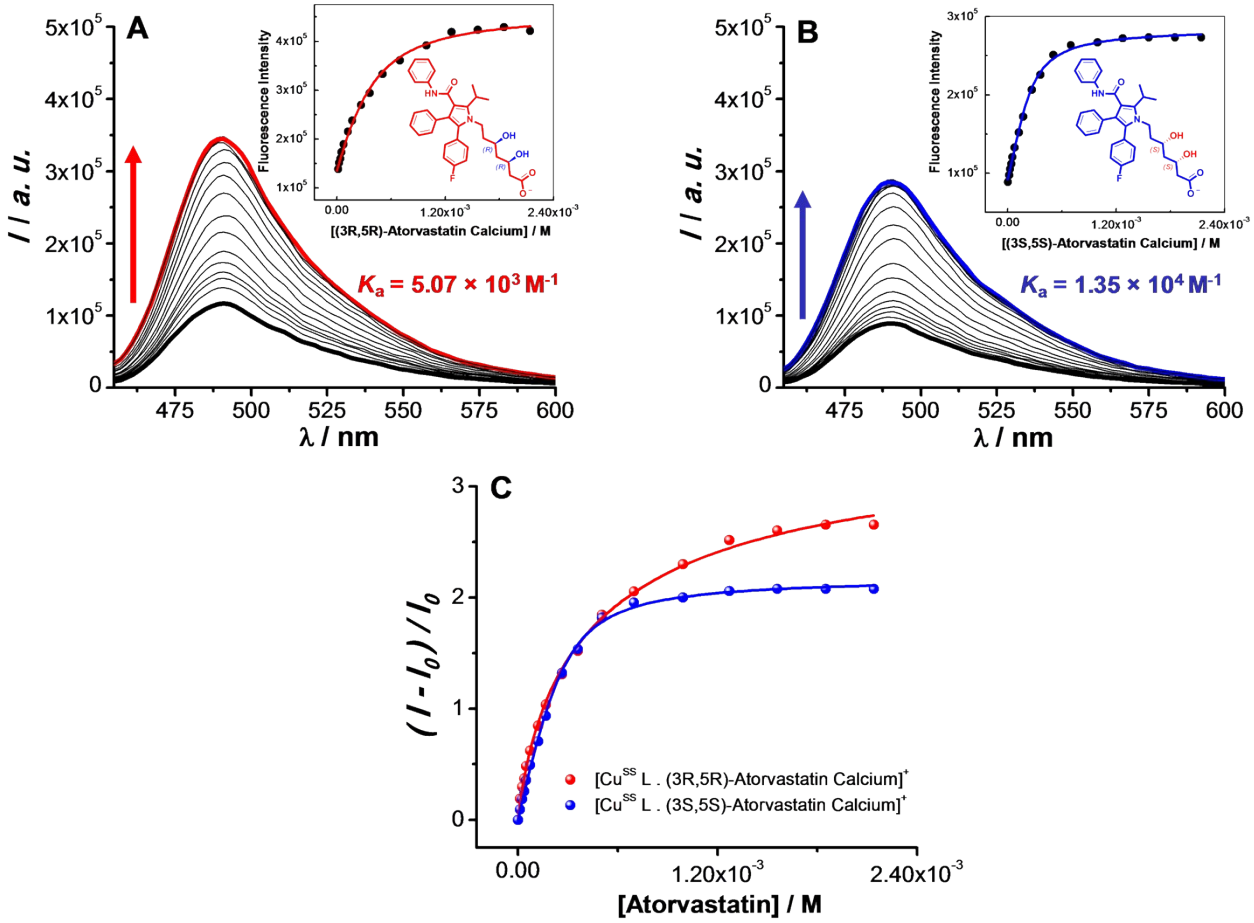

Figure S22. A) Titration profile of **[Cu^{SS}L•C343]$^{+}$** (212 µM) upon the addition of incremental amounts of **(*3R,5R*)-Atorvastatin calcium** in CH_3CN:H_2O 7:3 at pH= 6 (MES 50 mM). λ_{ex}= 444 nm. [(*3R,5R*)-Atorvastatin calcium]= 0–2.5 mM.

B) Titration profile of **[Cu^{SS}L•C343]$^{+}$** (212 µM) upon the addition of incremental amounts of **(*3S,5S*)-Atorvastatin calcium** in CH_3CN:H_2O 7:3 at pH= 6 (MES 50 mM). λ_{ex} = 444 nm. [(*3S,5S*)-Atorvastatin calcium]= 0–2.5 mM.

C) Titration isotherms based on the change in fluorescence intensity at the maximum wavelength of **[Cu^{SS}L•C343]$^{+}$** (212 µM) and partly enhanced upon the addition of incremental amounts of **(*3R,5R*)-Atorvastatin calcium** (red) and **(*3S,5S*)-Atorvastatin calcium** (blue) in CH_3CN:H_2O 7:3 at pH= 6 (MES 50 mM). λ_{ex} = 444 nm. [*(S)/(R)*-Atorvastatin calcium]= 0–2.5 mM.

[Cu^{RR}L•C343]$^{+}$ – Atorvastatin Calcium

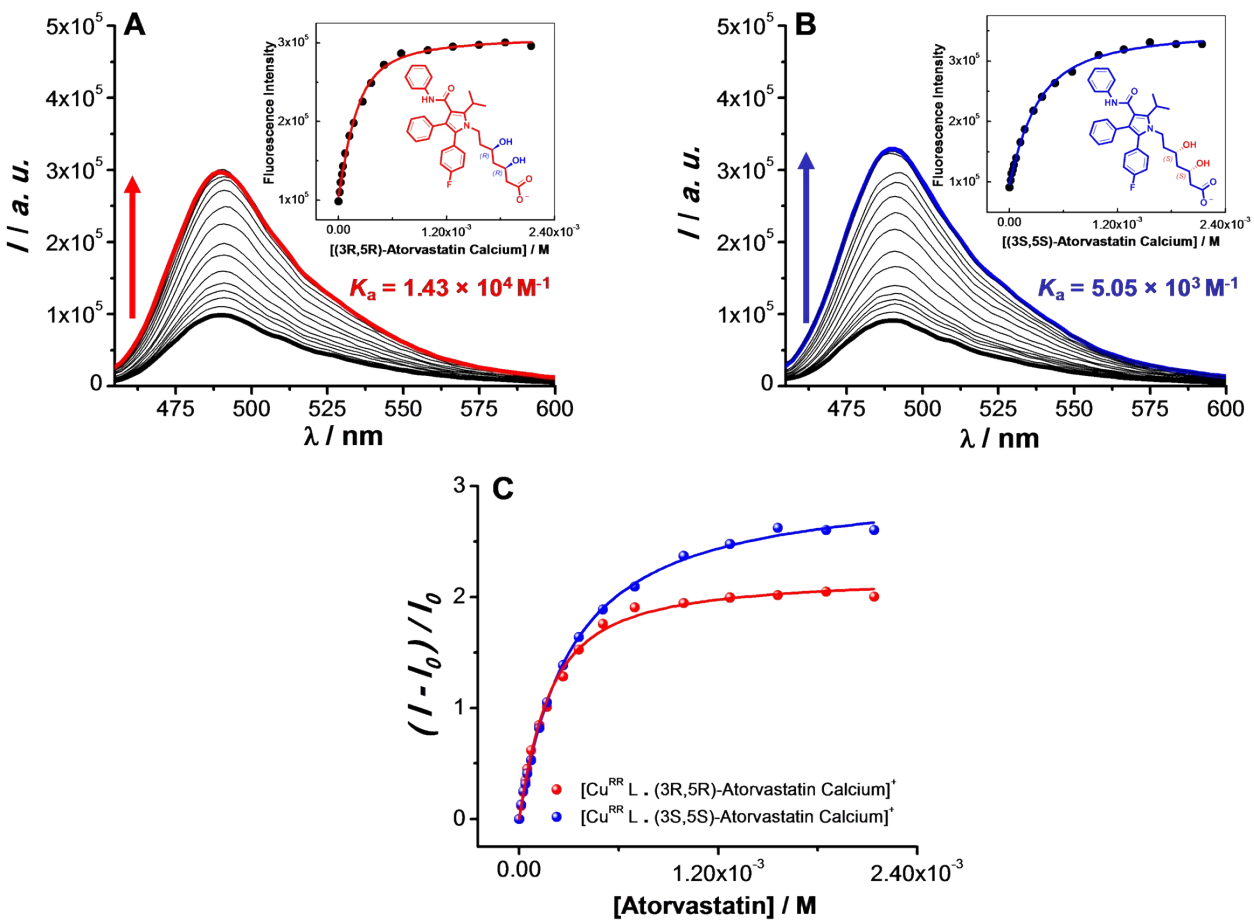

Figure S23. A) Titration profile of **[Cu^{RR}L•C343]$^{+}$** (212 μM) upon the addition of incremental amounts of **(*3R,5R*)-Atorvastatin calcium** in CH_3CN:H_2O 7:3 at pH= 6 (MES 50 mM). λ_{ex}= 444 nm. [(*3R,5R*)-Atorvastatin calcium]= 0–2.5 mM.

B) Titration profile of **[Cu^{RR}L•C343]$^{+}$** (212 μM) upon the addition of incremental amounts of **(*3S,5S*)-Atorvastatin calcium** in CH_3CN:H_2O 7:3 at pH= 6 (MES 50 mM). λ_{ex}= 444 nm. [(*3S,5S*)-Atorvastatin calcium]= 0–2.5 mM.

C) Titration isotherms based on the change in fluorescence intensity at the maximum wavelength of **[Cu^{RR}L•C343]$^{+}$** (212 μM) and partly enhanced upon the addition of incremental amounts of **(*3R,5R*)-Atorvastatin calcium** (red) and **(*3S,5S*)-Atorvastatin calcium** (blue) in CH_3CN:H_2O 7:3 at pH= 6 (MES 50 mM). λ_{ex}= 444 nm. [*(S)/(R)*-Atorvastatin calcium]= 0–2.5 mM.

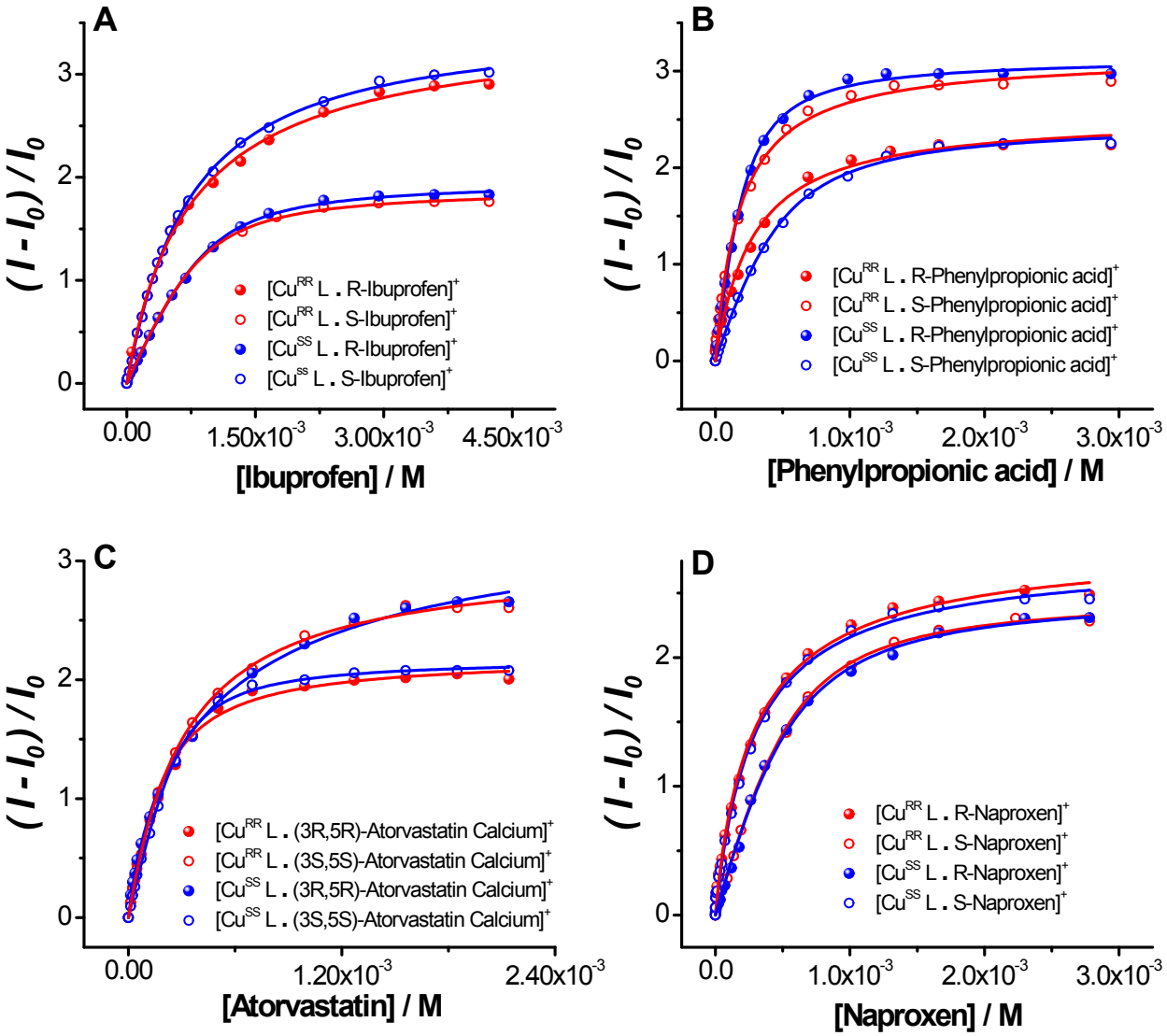
A
B
C
D
(I - I0) / I0
[Ibuprofen] / M
[Phenylpropionic acid] / M
[Atorvastatin] / M
[Naproxen] / M
[CuRR L . R-Ibuprofen]+
[CuRR L . S-Ibuprofen]+
[CuSS L . R-Ibuprofen]+
[Cuss L . S-Ibuprofen]+
[CuRR L . R-Phenylpropionic acid]+
[CuRR L . S-Phenylpropionic acid]+
[CuSS L . R-Phenylpropionic acid]+
[CuSS L . S-Phenylpropionic acid]+
[CuRR L . (3R,5R)-Atorvastatin Calcium]+
[CuRR L . (3S,5S)-Atorvastatin Calcium]+
[CuSS L . (3R,5R)-Atorvastatin Calcium]+
[CuSS L . (3S,5S)-Atorvastatin Calcium]+
[CuRR L . R-Naproxen]+
[CuRR L . S-Naproxen]+
[CuSS L . R-Naproxen]+
[CuSS L . S-Naproxen]+

Figure S24. Total titration isotherms based on the change in fluorescence intensity at the maximum wavelength of **[Cu^{RR}L•C343]$^{+}$** (red) and **[Cu^{SS}L•C343]$^{+}$** (blue) (212 μM) and partly enhanced upon the addition of incremental amounts of **(*R*)**-conformation and **(*S*)**-conformation **A)** Ibuprofen **B)** Phenylpropionic acid **C)** Atorvastatin calcium **D)** Naproxen in CH_3CN:H_2O 7:3 at pH= 6 (MES 50 mM). λ_{ex}= 444 nm.

[Cu^{SS}L•C343]$^{+}$ – Mandelic acid

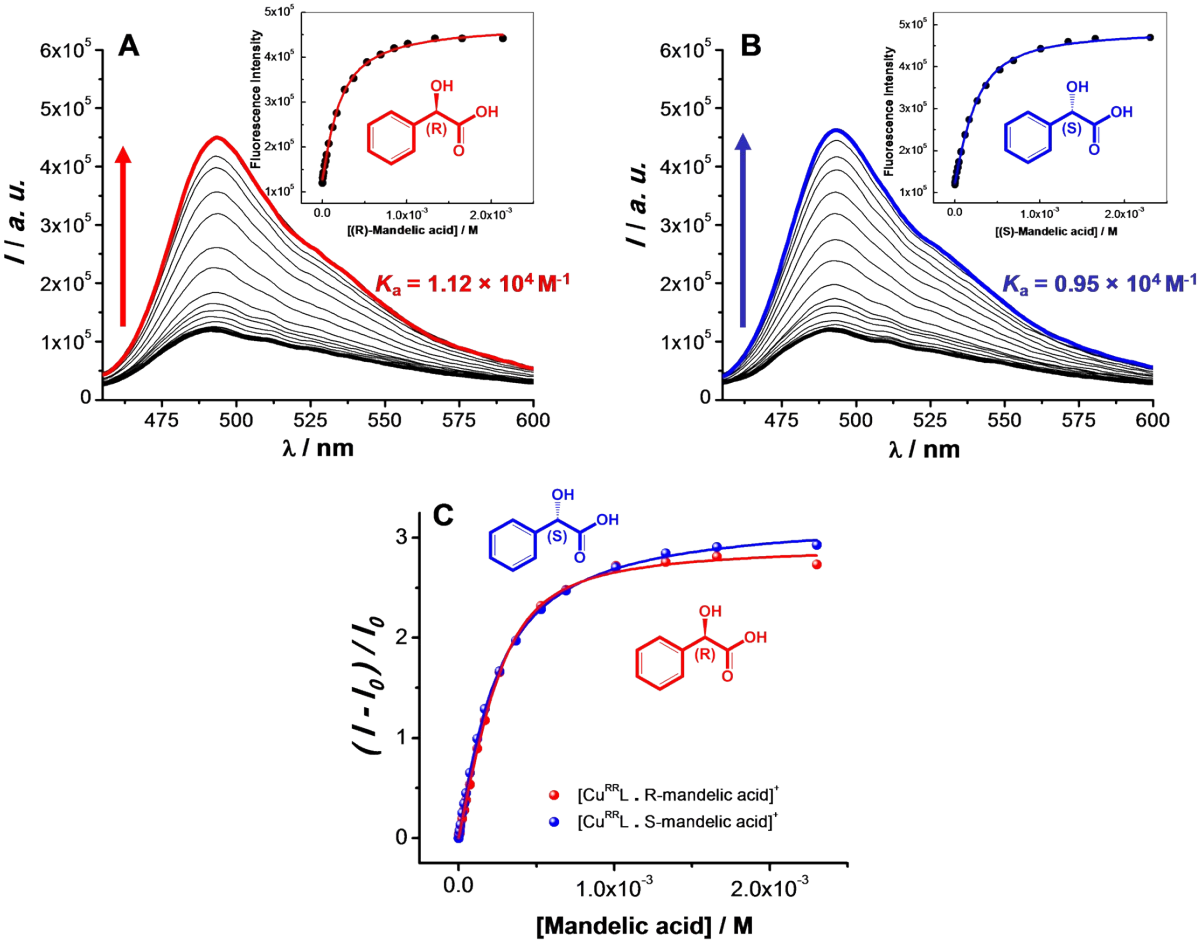

Figure S25. A) Titration profile of **[Cu^{SS}L•C343]$^{+}$** (212 μM) upon the addition of incremental amounts of **(*R*)-Mandelic acid** in CH_3CN:H_2O 7:3 at pH= 6 (MES 50 mM). λ_{ex}= 444 nm. [(*R*)-Mandelic acid]= 0–2 mM.

B) Titration profile of **[Cu^{SS}L•C343]$^{+}$** (212 μM) upon the addition of incremental amounts of **(*S*)-Mandelic acid** in CH_3CN:H_2O 7:3 at pH= 6 (MES 50 mM). λ_{ex}= 444 nm. [(*S*)-Mandelic acid]= 0–2 mM.

C) Titration isotherms based on the change in fluorescence intensity at the maximum wavelength of **[Cu^{SS}L•C343]$^{+}$** (212 μM) upon the addition of incremental amounts of **(*R*)-Mandelic acid** (red) and **(S)-Mandelic acid** (blue) in CH_3CN:H_2O 7:3 at pH= 6 (MES 50 mM). λ_{ex}= 444 nm. [*(S)/(R)*-Mandelic acid] = 0–2 mM. There is no appreciable difference between the isotherms and no statistical difference between the binding constants.

[Cu^{SS}L•C343]$^{+}$– Lactic acid

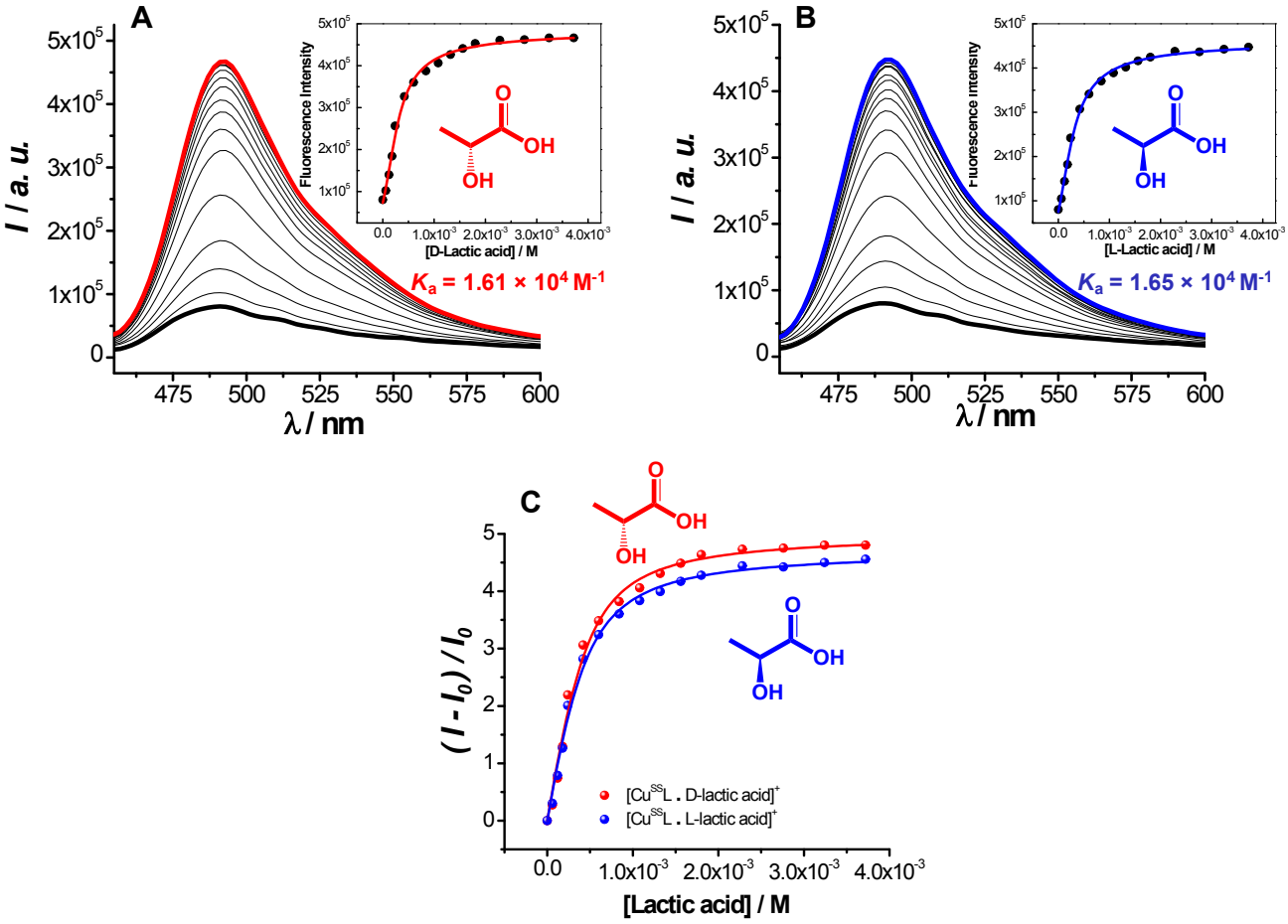

Figure S26. A) Titration profile of **[Cu^{SS}L•C343]**$^{+}$ (212 μM) upon the addition of incremental amounts of ***(D)*-lactic acid** in CH_3CN:H_2O 7:3 at pH= 6 (MES 50 mM). λ_{ex}= 444 nm. [*(D)*-lactic acid]= 0–4 mM.

B) Titration profile of **[[Cu^{SS}L•C343]**$^{+}$ (212 μM) upon the addition of incremental amounts of ***(L)*-lactic acid** in CH_3CN:H_2O 7:3 at pH= 6 (MES= 50 mM). λ_{ex}= 444 nm. [*(L)*-lactic acid] = 0–4 mM.

C) Titration isotherms based on the change in fluorescence intensity at the maximum wavelength of **[Cu^{SS}L•C343]**$^{+}$ (212 μM) upon the addition of incremental amounts of ***(D)*-lactic acid** (red) and ***(L)*-lactic acid** (blue) in CH_3CN:H_2O 7:3 at pH= 6 (MES 50 mM). λ_{ex}= 444 nm. [*(D)/(L)*-lactic acid]= 0–4 mM. There is no appreciable difference between the isotherms and no statistical difference between the binding constants.

[Cu^{SS}L•C343]$^{+}$ – 3-phenyllactic acid

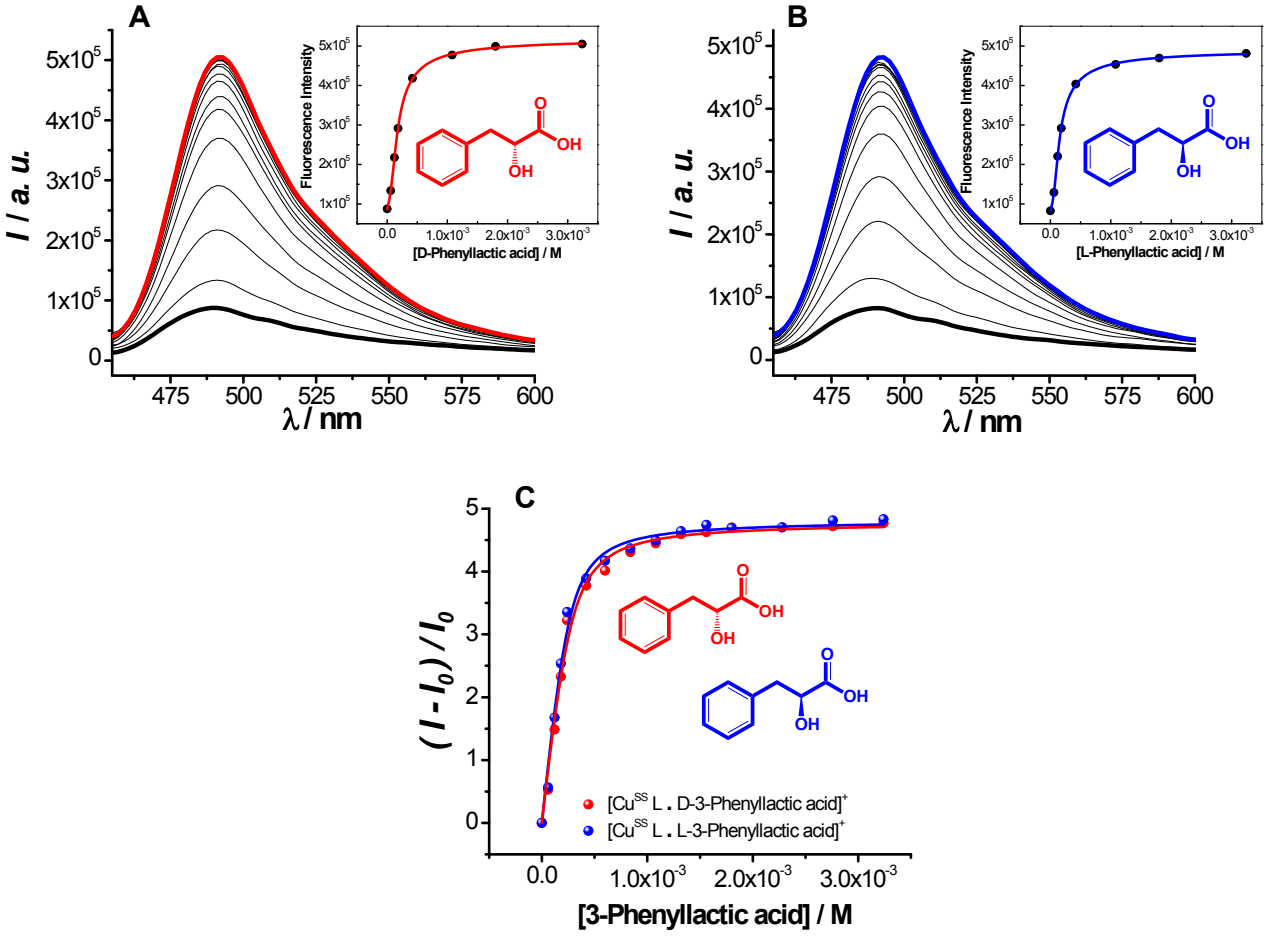

Figure S27. A) Titration profile of **[Cu^{SS}L•C343]**$^{+}$ (212 μM) upon the addition of incremental amounts of ***(D)*-3-phenyllactic acid** in CH_3CN:H_2O 7:3 at pH= 6 (MES 50 mM). λ_{ex}= 444 nm. [*(D)*-3- phenyllactic acid]= 0–3.5 mM

B) Titration profile of **[Cu^{SS}L•C343]**$^{+}$ (212 μM) upon the addition of incremental amounts of ***(L)*-3-phenyllactic acid** in CH_3CN:H_2O 7:3 at pH= 6 (MES 50 mM). λ_{ex} = 444 nm. [*(L)*-3-phenyllactic acid] = 0–3.5 mM.

C) Titration isotherms based on the change in fluorescence intensity at the maximum wavelength of **[Cu^{SS}L•C343]**$^{+}$ (212 μM) upon the addition of incremental amounts of ***(D)*-3-phenyllactic acid** (red) and ***(L)*-3-phenyllactic acid** (blue) in CH_3CN:H_2O 7:3 at pH= 6 (MES 50 mM). λ_{ex}= 444 nm. [*(D)*/*(L)*-3-phenyllactic acid]= 0–3.5 mM. There is no appreciable difference between the isotherms and no statistical difference between the binding constants.

6. UV-Vis titrations

All solutions were prepared in $CH_3CN:H_2O$ 7:3 at pH= 6 (MES= 50 mM). [Sensors]= 1 mM

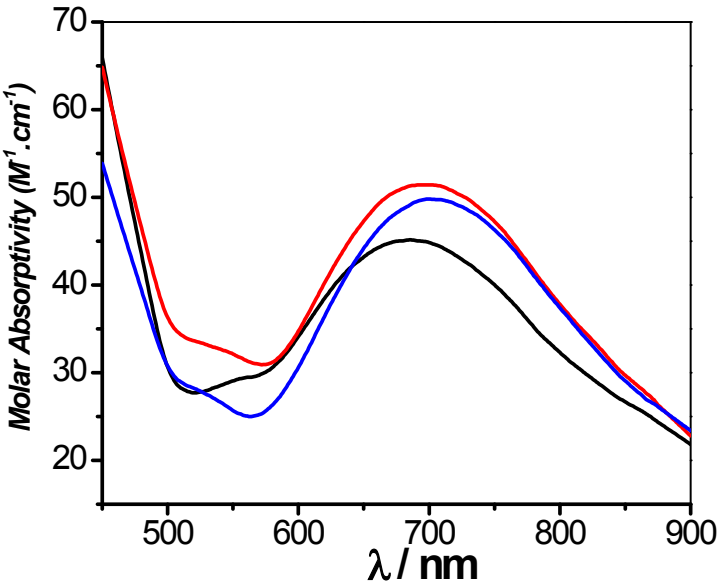

Figure S28. Titration spectra of **[Cu^{SS} L]$^{2+}$** (1 mM) upon the addition of incremental amounts of **(*R*)-phenylpropionic acid** in $CH_3CN:H_2O$ 7:3 at pH= 6 (MES 50 mM). [(*R*)-phenylpropionic acid]= 0–3 equivalents. Black: 0 equiv. Red: 1 equiv. Blue: 3equiv.

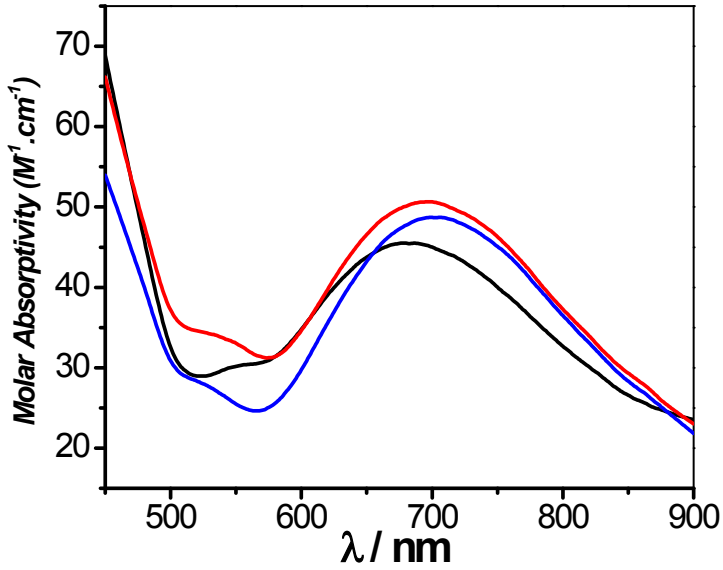

Figure S29. Titration spectra of **[Cu^{SS} L]$^{2+}$** (1 mM) upon the addition of incremental amounts of **(*S*)-phenylpropionic acid** in $CH_3CN:H_2O$ 7:3 at pH= 6 (MES 50 mM). [(*S*)-phenylpropionic acid]= 0–3 equivalents. Black: 0 equiv. Red: 1 equiv. Blue: 3equiv.

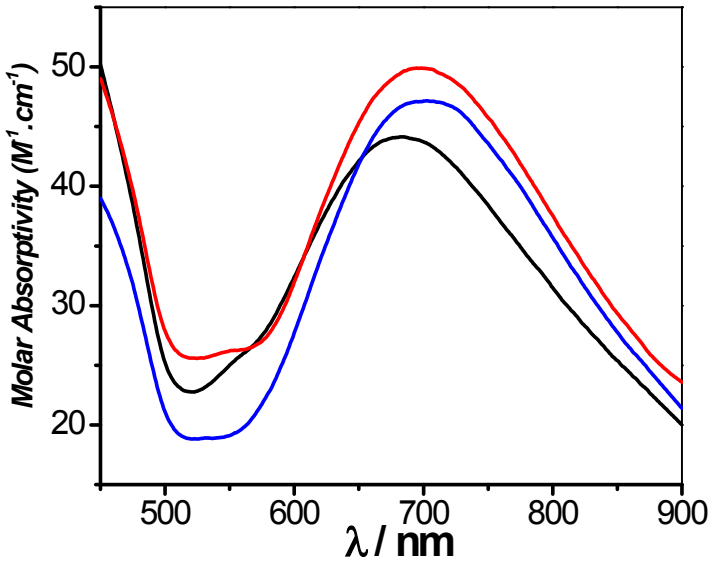

Figure S30. Titration spectra of **[Cu^{RR} L]$^{2+}$** (1 mM) upon the addition of incremental amounts of **(*R*)-phenylpropionic acid** in CH_3CN:H_2O 7:3 at pH= 6 (MES 50 mM). [(*S*)-phenylpropionic acid]= 0–3 equivalents. Black: 0 equiv. Red: 1 equiv. Blue: 3equiv.

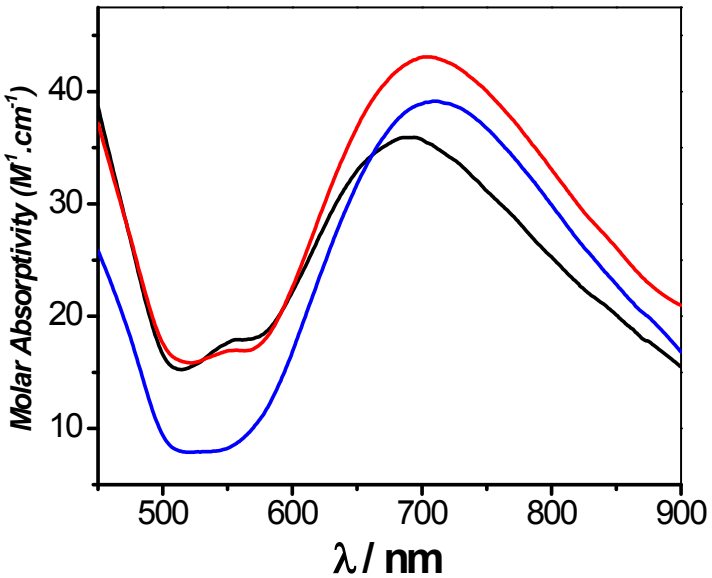

Figure S31. Titration spectra of **[Cu^{RR} L]$^{2+}$** (1 mM) upon the addition of incremental amounts of **(*S*)-phenylpropionic acid** in CH_3CN:H_2O 7:3 at pH= 6 (MES 50 mM). [(*S*)-phenylpropionic acid]= 0–3 equivalents. Black: 0 equiv. Red: 1 equiv. Blue: 3equiv.

7. Stoichiometry determination: Job's plot

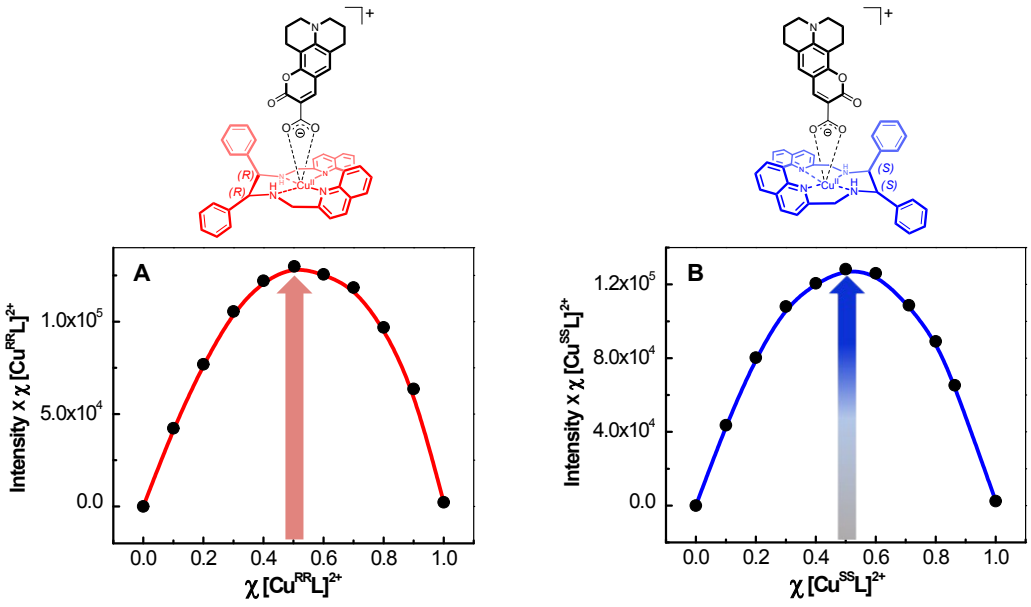

Figure S32. Job's plot for the determination of the stoichiometry of **A)** $[Cu^{RR}L)]^{2+}$ and Coumarin 343; **B)** $[Cu^{SS}L)]^{2+}$ and Coumarin 343 in $CH_3CN:H_2O$ 7:3 at pH= 6 (MES 50 mM).

8. Dependence of fluorescence intensity on *ee*: Standard curve experiment

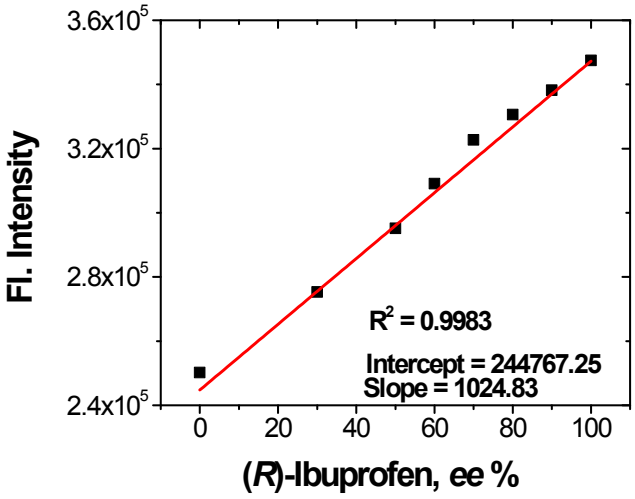

Figure S33. Standard curve for fluorescence (Fl) intensity reading obtained from a binary mixture of *R*- and *S*-enentiomers of ibuprofen with known *ee*. The resulting graph of Fl vs. *ee* is linear and therefore absolute configuration and *ee* of unknown sample can be determined by interpolation of their fluorescence reading on the graph.